REPUBLIC OF TÜRKİYE

ALTINBAŞ UNIVERSITY

Institute of Graduate Studies

Information Technologies

SEGMENTATION OF BRAIN TUMOR MRI IMAGES USING WATERSHED THRESHOLDING

Ahmed Talib Atiyah ATIYAH

Master's Thesis

Supervisor

Prof. Dr. Osman Nuri UÇAN

Istanbul,2022

SEGMENTATION OF BRAIN TUMOR MRI IMAGES USING WATERSHED THRESHOLDING

Ahmed Talib Atiyah ATIYAH

Information Technologies

Master's Thesis

ALTINBAŞ UNIVERSITY

2022

The thesis titled SEGMENTATION OF BRAIN TUMOR MRI IMAGES USING WATERSHED THRESHOLDINGprepared by AHMED TALIB ATIYAH ATIYAH and submitted on 09/12/2022 has been **accepted unanimously** for the degree of Master of Science in Information Technologies.

____

Prof. Dr. Osman Nuri UÇAN

the Supervisor

Thesis Defense Committee Members:

Prof. Dr. Osman Nuri UÇAN	Department of Electrical and Electronics Engineering, Altınbaş University	__________________
Asst. Prof. Dr. Sefer KURNAZ	Department of Computer Engineering, Altınbaş University	__________________
Assoc. Prof. Dr. Adil Deniz DURU	Department of Trainer Education, Marmara University	__________________

I hereby declare that this thesis meets all format and submission requirements of a Master's thesis.

Submission data of the thesis to Institute of Graduate Studies: ____/____/____

I hereby declare that all information and data presented in this graduation project has been obtained in full accordance with academic rules and ethical conduct. I also declare all unoriginal materials and conclusions have been cited in the text and all references mentioned in the Reference List have been cited in the text, and vice versa as required by the abovementioned rules and conduct.

Ahmed Talib Atiyah ATIYAH

Signature

ACKNOWLEDGEMENTS

To those whose soul has not left me. For you Mom, because you are gone. I really wish I could have kept you longer to see that achievement.

To Iman ALTEWAIG, words alone cannot convey the amount of gratitude I hold for your infinite giving.

To Osool ATIYAH My friends, my love, my sister, the main moral supporter and the second mother, thank you, the size of a galaxy.

To Diaa JAWAD The absent, yet present in every moment, the first to encourage me thank you.

To my great advisor Prof. Dr. Osman Nuri UÇAN Thanks for the continuous follow up.

To Ali JAWAD, Abdulla ABBAS When we are together, we don’t know the word impossible, thanks a lot my best friend.

ABSTRACT

SEGMENTATION OF BRAIN TUMOR MRI IMAGES USING WATERSHED THRESHOLDING

Atiyah, Ahmed Talib Atiyah

M.Sc., Information Technologies, Altınbaş University,

Supervisor: Prof. Dr. Osman Nuri UÇAN

Date: 12/2022

Pages: 95

The detection of brain tumors using magnetic resonance imaging (MRI) brain scans has become one of the most active areas of research in the field of medical image processing. The primary purpose of the system is the detection of the tumor. In biomedical imaging, detection plays a pivotal function. In this study, MRI brain images are used to detect tumors. If a clear image of the brain cannot be obtained and the location, size, and type of the tumor are known, the patient will be administered incorrect doses, resulting in the destruction of healthy brain tissue. Due to the dearth of radiology-trained physicians, which lengthens the time required to make a diagnosis due to the doctors' workload, the algorithm's ability to reduce the time and speed required to make a diagnosis makes it extremely valuable if implemented. In this study we propose a new method for segmenting the tumor territory on MRI scans in order to locate and isolate it. Initially, the watershed approach is used to the images, followed by a second segmentation to isolate the brain tumor. MATLAB and Maya will be utilized for all application and division activities. After including a fitness function into the algorithm, the DICE- and JACCARD-segmented images will be scored to determine how well they compare to one another. When a 0.1 mm threshold was applied to either process, the resulting accuracy was outstanding. When comparing the results of the 3D segmentation to those of other models using interscan evaluation, discrepancies more than 0.1 mm were observed in 16 of 21 instances. If other brain tumor segmentation algorithms use the standard threshold for segmentation, they will miss areas of the tumor. By modifying the segmentation threshold, we were able to recreate previously nonexistent brain regions and assess how these alterations affected the image quality. Both the Jaccard and Dice segmentation scores hit an all-time high of 0.95 after the threshold change.

Keywords: Brain Tumor, Watershed Algorithm, Image Segmentation, MRI.

TABLE OF CONTENTS

Pages

LIST OF TABLES

Pages

LIST OF FIGURES

Pages

ABBREVIATIONS

CT	:	Computed Tomography
MRI	:	Magnetic Resonance Imaging
FCM	:	Fuzzy Clustering Method
PD	:	Proton Density
LoG	:	Laplacian Of Gaussian
GLCM	:	Gray Level Co-Occurrence Matrix

1. INTRODUCTION

1.1 BACKGROUND

Digital imaging technology is becoming increasingly prevalent in the modern world, and the number of scientific disciplines that could profit from it is constantly expanding. A variety of picture altering applications have recently gained favor as efficient tools for enhancing image analysis. This tendency is anticipated to persist. By doing an analysis on the values and dimensions of each segment, a segmentation technique can be utilized to manage an image object more efficiently. Digital imaging has become increasingly important in the medical profession, with many research opting to analyze digital images in magnetic resonance imaging (MRI) format. Image analysis, pattern recognition, and even blind perception can greatly benefit from image segmentation [1]. Segmentation is largely applied to increase image analysis and comprehension by dividing an image into portions based on one or more criteria, such as color and object. This is achieved by separating the image into segments. The watershed algorithm is only one example of the countless methods and techniques that have been proposed in relation to segmentation. This picture partitioning technique has a range of potential uses, including medical image analysis. [2] Medical image segmentation is a crucial component of this study field. Object recognition in medical images, such as those of the brain, heart, and kidneys, relies heavily on a pre-processing technique referred to as "edge detection" of the underlying medical images. This method is used to determine the boundaries of anatomical structures.

1.1.1 Medical Imaging

Radiological imaging techniques such as computed tomography (CT), magnetic resonance imaging (MRI), and x-ray can be used to provide anatomically accurate images of internal organs. Other imaging techniques include ultrasonography and nuclear medicine. These photos are essential for medical diagnosis, medical education, and medical research. It is difficult to detect internal organs in these photos due to either the presence of noise or the irregular shape of the human body's components. Due to the fact that images obtained from magnetic resonance imaging (MRI) are now extremely useful in the diagnostic process, image processing and segmentation techniques have become indispensable in the field of medical research. This is because the borders within human organs and tissues can only be defined by closely examining images such as these.

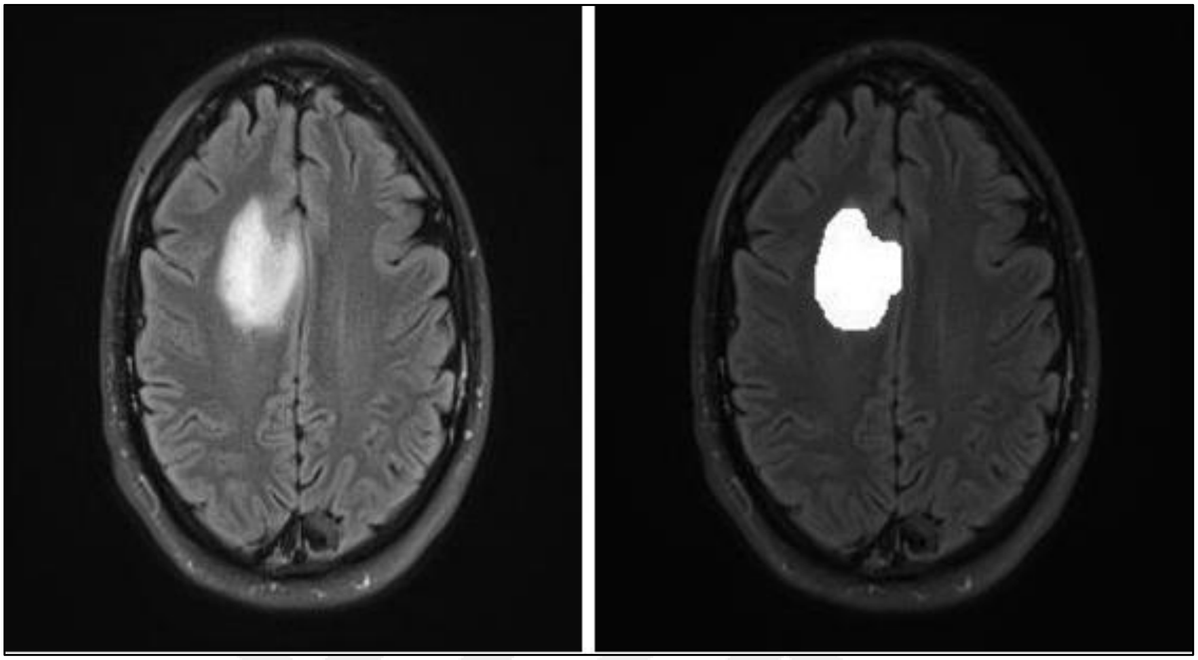

Figure 1.1: Brain tumor definition in MRI Using segmentation [44].

1.1.2 MRI Image Segmentation

This is possible with grayscale, RGB, and multidimensional images such as MRI scans. The purpose of segmentation is to extract usable information for statistical reasons about the thing being segmented, as well as to classify and analyze the segmented object. The segmentation approach, which includes dividing an image into usable pieces, is one of the subfields that lie under the umbrella of digital image processing. When attempting to prevent excessive segmentation, a problem that affects a number of segmentation algorithms, the initial step is frequently a smoothing or filtration technique to reduce noise. This issue happens when the image contains unwanted information (noise) that the algorithm perceives mistakenly as a segment. The marker controller allows for the elimination of unneeded levels of segmentation. When attempting to identify an MRI image, aspects such as image quality, picture size, color contrasts, and image dimensions should be addressed. These are merely few of the many aspects. The watershed transforms for tumor segmentation, also known as the region-based segmentation methodology, is one of the many techniques that have been utilized to segment tumors over the past decade. This method relies on the use of water to inundate the desired landscape or geographical relief. When all low regions are saturated with water from a variety of water sources at their respective local minima, which is the lowest point in the water catchment, the watershed is the line that divides the rainwater-collecting water catchments. The watershed is the line separating the water catchments. Once basins have formed between each zone, showing the locations of the highest regions and peaks, the process will be complete. A multidimensional image is reduced to a one-dimensional image when a picture is segmented using grayscale mathematical morphological watersheds. Recognizing basins and pinpointing specific areas by identifying seed are the two most crucial tactics for the transformation of watersheds.

1.1.3 MRI Segment Classifications

The diagnosing result whether the segment refer to a benign tumor or a malignant one. The four inputs for the function are area, color contras, position of segment in the lower part of the brain and the position on the upper part. These features are the member functions to make the final conclusion which allows representing the relations between tumor and surrounding tissue. All processing steps are performed in 3D type of gray scale images.

1.2 PROBLEM STATEMENT

a. When a cancerous tumor in the brain is diagnosed incorrectly or slowly, it will result in many problems, including aggravation of the patient's condition, spread of disease, and death. In the event that a clear image of the brain is not seen, and the location, size and type of the tumor are known, the patient will be given wrong doses, causing damage to healthy brain tissue.
b. Due to the scarcity of doctors specialized in radiology, which delays the diagnosis time due to the momentum of doctors, the algorithm is of great importance in reducing the time and speed of diagnosis, which makes it very useful if used.

1.3 THESIS OBJECTIVES

1.3.1 General Objective

The fundamental objective of the watershed and threshold technique is to locate and localize the tumor within the patient's brain. This cutting-edge technology will find a brain tumor in three easy steps, and then divide it into manageable pieces based on its locations. Utilizing segmentation and morphological operators, we will discuss an approach for finding malignancies that is highly effective. After improving the quality of the scanned image, morphological operators will be applied to pinpoint the exact site of the tumor. Prior to beginning segmentation, an operation will be performed to improve the picture quality and reduce the possibility of overlap between previously divided regions.

1.3.2 Specific Objectives

The specific objectives of this work are listed below:

i. Segmentation of brain tumor MRI in different modalities.
ii. Improvement of Watershed method using an image enhancement technique.
iii. Implementation of the proposed system on MATLAB r2022a.
iv. Evaluation of the proposed method using similarity indices such as Dice index and Jaccard similarity index.

1.4 CONTRIBUTION

When working with complex medical images, segmentation is necessary for determining the region of interest for further analysis. As a result of segmenting the complete tumor profile, the initial population was very vast; however, this has been drastically decreased so that focus may be directed on a more restricted genetic group. This study's primary contribution is a reliable approach for segmenting the tumor territory on MRI scans to find and isolate it. First, the watershed method is used to the images, followed by a second segmentation in order to obtain the brain tumor. After including a fitness function into the algorithm, we will score the DICE and JACCARD-segmented images to assess how well they compare to one another.

1.5 THESIS STRUCTURE

The thesis consists of six chapters. The first chapter is an introduction.

The rest of the thesis contains four chapters they are as follows:

a. Chapter Two presents state of the art methods and previous works done on this subject.
b. Chapter three introduces theoretical background related to our proposed model
c. Chapter four will present the design and implementation of the MRI segmentation using 3D Watershed algorithm.

d. Chapter five presents the simulation results and comparison with the literature
e. Finally in chapter six we will conclude our work and presents recommendations for future work.

2. LITERATURE REVIEW

2.1 CHAPTER INTRODUCTION

Digital photography technology has become a vital part of modern life, and it has contributed to the advancement of many scientific areas. Many images altering software's have recently arisen and been launched as tools to advance image analysis. A segmentation method is required to analyze the values and measurements of each segment in order to manage an item that is part of an image. Digital imaging has becoming more important, particularly in medical domains; researchers in this sector prefer to analyze digital images in (MRI) form. To simplify its representation, a digital image may be segmented, which means that its pixels may be separated into smaller groups. There are a variety of methods for separating data. Thresholding is a method that converts an input grayscale image into a binary image depending on a threshold value. There are two kinds of thresholding. (a) Global (b) Regional Watershed transformations arrange pixels in a image based on their intensities.

2.2 IMAGE SEGMENTATION

The segmentation method allows an image to be divided into a large number of subsections (Sets of pixels). The purpose of segmentation is to simplify the representation of an image in order to facilitate subsequent modification and analysis. This is achieved by deleting unneeded elements from the image. In order to accomplish this, we will crop the image to remove any extraneous parts. If the foreground is defined at a high-level grade and the segments are identified at a lower-level grade, picture segmentation can be understood as the process of abstracting an object from an image. This is done in order to get the desired result. It is recommended that a digital photograph be split into two individual images. The first phase in the process is called pre-processing, and it involves analyzing the (input image) to determine its size, quality, color density, type, and noise levels, among other characteristics. When seen from the opposite angle, the piece of the image that is wanted may be cut out of that image by determining the value of the (outgoing) segment in comparison to the work that was originally created. This chapter will discuss a number of the many methods of segmentation that have been created over the course of the preceding decades. One of these methods, the suggested algorithm watershed, will be among those discussed.

2.2.1 Threshold Based Segmentation

Methods for slicing may be applied directly to a digital image, or they may be included into further pre-processing or post-processing techniques. In any case, they are helpful. In this methodology, the histogram thresholding method is used.

$$g(t) = \begin{cases} 0 \; if \; t < s \\ 1 \; if \; t > s, \end{cases} \tag{2.1}$$

Where (t) represent time period and (s) represent the threshold value, the equation above shows us two thresholds used which is binary. Using multiple thresholds can also implement, that gives us more detailed segmentation as shown in equation (2.2)

$$g(t) = \begin{cases} 0 \text{ if } t < s1 \\ 1 \text{ if } s1 \leq t < s2 \\ 2 \text{ if } s2 \leq t < s3 \\ . \\ . \\ . \\ n \text{ if } s1 \leq tn < t \end{cases} \tag{2.2}$$

As shown in Figure (2.1), the four images (a, b, c and d) show using multiple thresholds at the same image any un expert person can see the difference with the four images.

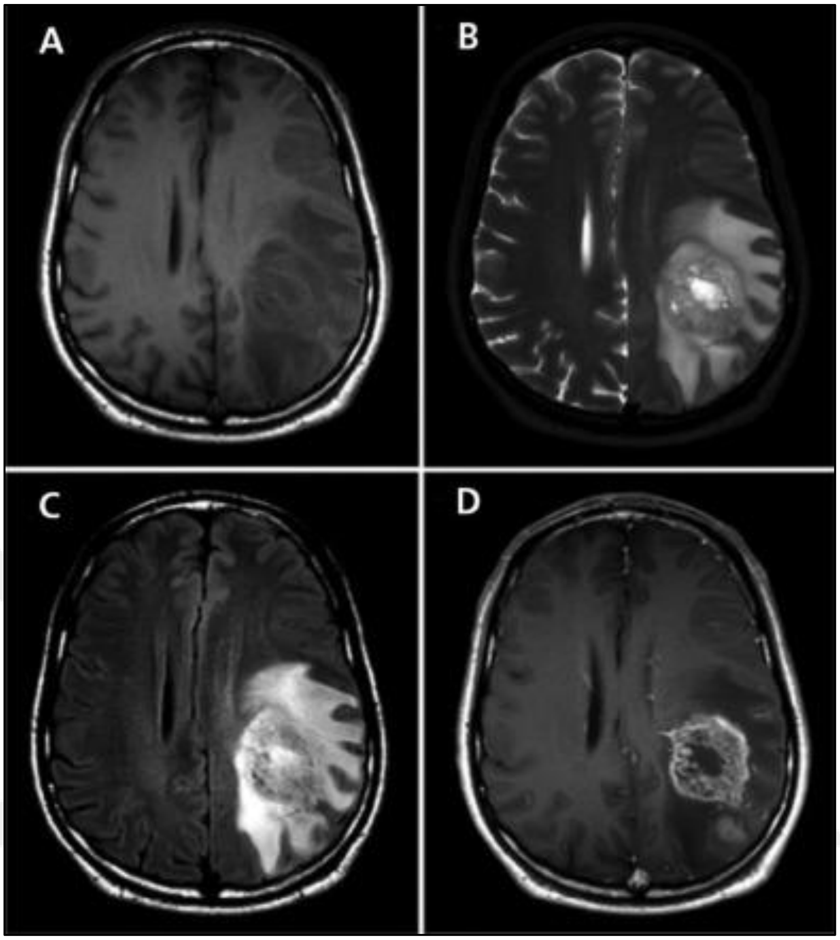

Figure 2.1: Using multiple segment (A) image. (B) Result after applying a low threshold value to segment the image into head and background pixels (C) Result after applying a higher value to segment the bone (D) result after applying both thresholds at the same time [31].

2.2.2 Region Growing Segmentation

This procedure starts inside the object and grows until it reaches the segment boundaries. This is accomplished in the other manner of how the edge method segmentation works, which is to detect edges and boundaries and put them together in order to locate an item. This technique likewise starts inside the object and grows until it reaches the segment boundaries [12].

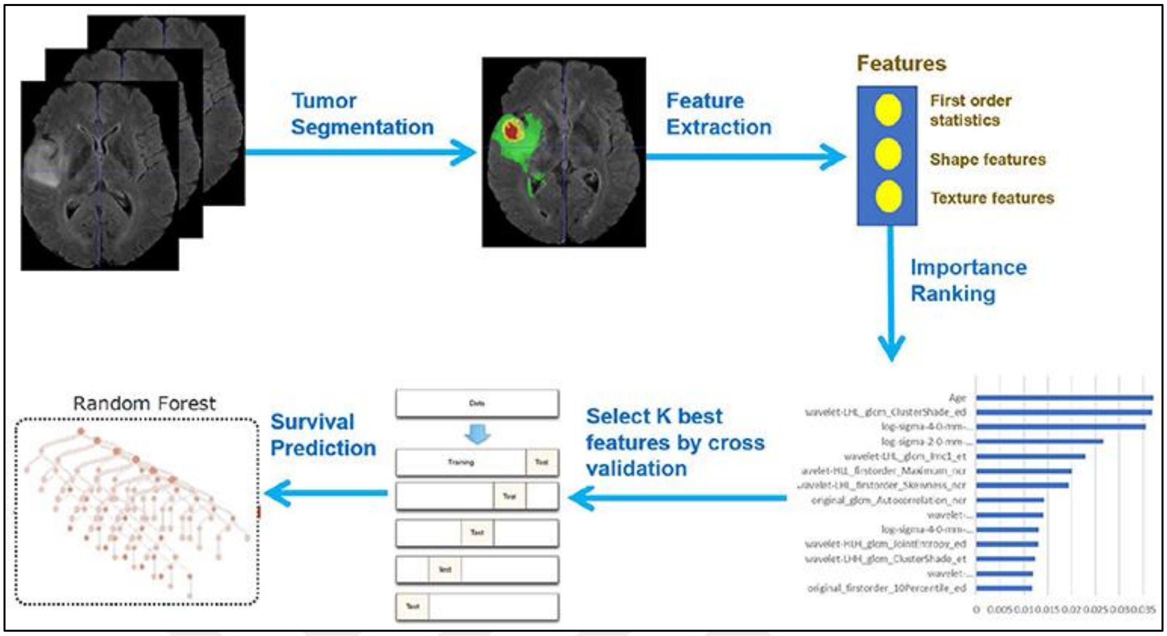

Figure 2.2: Region growing brain tumor segmentation technique [4].

2.2.3 Edge Detection

For the sake of this discussion, we will refer to this phenomenon as "image intensity changes from one pixel to the next." Image segmentation can be simplified and made more efficient by focusing mostly on an image's edges as opposed to other image characteristics.

Mathematical approaches are utilized to locate and determine the positions of numerous spots within an image that exhibit fast brightness changes. This technique is known as edge detection. A line or curve created by a collection of pixels in an image is of great aid to the process of image segmentation.

Utilizing the image's gradient derivatives to determine the image's derivatives is the most well-known approach for finding edges in an image. However, there are further approaches that may be utilized to do this. When calculating second-order derivatives, the Laplacian method is the preferred method. Canny, Sobel, and Prewitt are a few of the several approaches used [13].

2.2.4 Watershed Segmentation

Since its inception in 1979, The watershed method has been widely utilized in the field of image processing, specifically for the purpose of image segmentation. This is particularly true. Since its start, the circumstance has been consistent the vast percentage of the time. Depending on your perspective, the watershed technology can be understood as either an algorithm or a physical component. First, we shall mark the thesis watershed in situ in order to build a highly accurate section. The section will then be generated by superimposing the updated watershed on top of the prior watershed. This is the course of action we will follow to guarantee that our contribution is as precise and accurate as necessary.

The word "watershed" first appeared by researchers in regard to the natural environment. To totally submerge the land, water sources were deliberately positioned at each of the minimum locations of the relief. After the confluence of water sources, barriers will be created.

The inclusion of morphological watersheds, which are used to divide the analyzed items, considerably improves this method. Its only function is to separate things that are positioned in close proximity.

While the gray landscape is being flooded from all sides, catchment basins are being built and the watershed's borders are being established. After applying this method to grayscale images, the final output will have discernible edges. Images are likely to be over segmented in the vast majority of situations. This is particularly true for images containing a substantial amount of noise, such as CT and MRI scans. Either the image must be reprocessed, or portions of the image must be joined with pieces from other sites that fulfil the same specifications [14].

2.2.5 Watershed Segmentation Using Marker Controller

Most often, the watershed transform is used to separate items that are positioned in close proximity to one another in an image. This is performed by detecting the border "catchment basins," where bright images indicate elevated regions and dark pixels indicate low surfaces. Both the positions of items in the front and the backdrop are "marked" by watershed. There are just a few simple steps to take [14]:

a. Determine the purpose of segmentation in the dark pixels in a digital image.
b. The foreground markers should be computed. The object's interconnected pixels.
c. The background marker is calculated. Non-objective pixels may be found here.
d. Calculate the changed function's watershed transform.
e. It is necessary to remove any minima from the foreground and background before using this step's segmentation function.

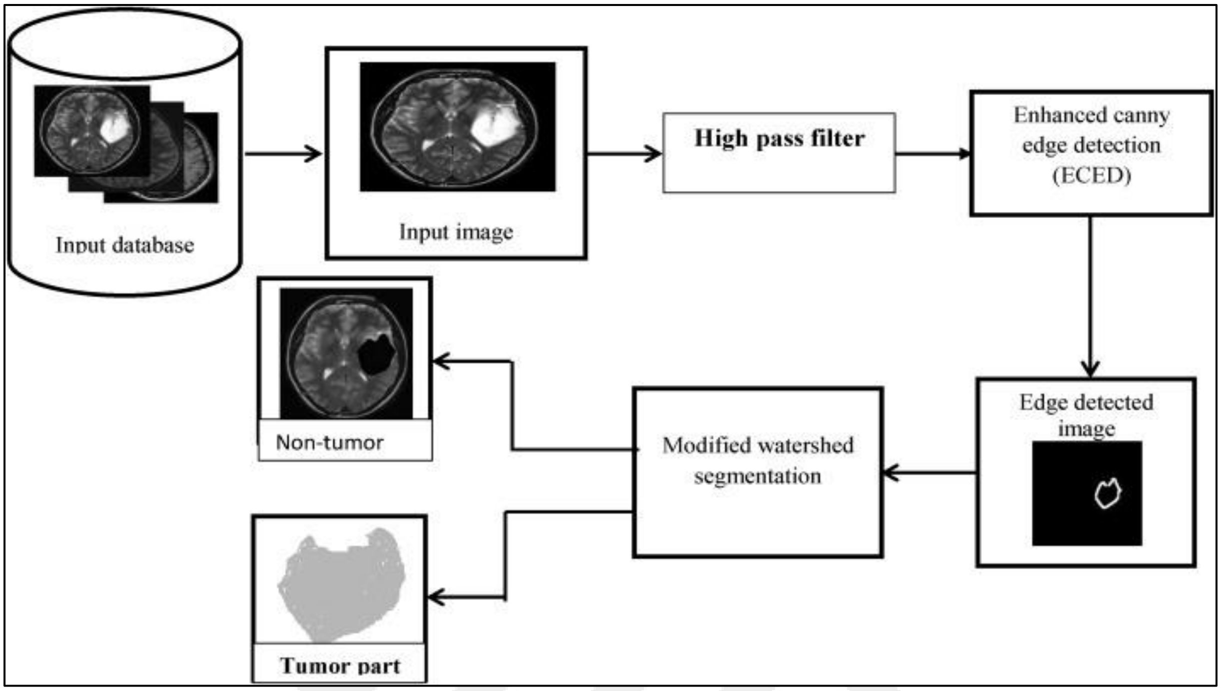

Figure 2.3: Watershed segmentation for brain tumor MRIs [1].

2.3 LITERATURE SURVEY

In the following, some proposals have been drawn from the scientific literature:

a. S. Deepak et al. [1] utilizing the same information source as mentioned in [2], the photos were categorized using the "deep remove" method. Eliminate the image's functions and instead include them into your experimental and classification models. Utilizing a 5-classification technique, the author was able to achieve a 98% success rate at the patient level. Automatic categorization was more advantageous to the organization of regions than conventional urban classification, according to the study's conclusions.

b. Another study by Afshar et al. [2] Utilizes a CapsNet-based model of brain tumors as a classification model of Capsule networks. The study improves accuracy by integrating CapsNet mapping tweaks into chosen convolutional layers.

c. According to the study of [3], using deep learning methods on brain tumor segmentation and classification, the accuracy can increase significantly with feature selection methods.

d. Another study by Abiwinanda et al. [4] Convolutional neural networks were used to develop a deep learning model that was used to assess images of brain cancers. The research used a total of five distinct classification models, with finding 2 proving to be the most effective. The structure is completed by either a RELU layer or a pool layer. There are sixty-four dormant neurons within this sheltered area. If it uses what it has learned in class, it is expected to pass the program with a competency rate of 98.5% and obtain certification with a success rate of 84.19 percent. Utilizing two-dimensional contrast pedestals based on wavelet and Gabor filters, [5] investigates the usefulness of brain MRI using wavelet and Gabor filters. During the trial, the employment of the aforementioned technique in conjunction with NN backpropagation generated 91.9% accurate readings.

e. Pashaei et al. [6] WE designed a technique for feature mining that was based on CNN's methodology. In addition, they developed a novel three-layer arrangement and a five-layer architecture in which each layer served as a learning layer. CNN's baseline ELM-based classification model was predicted to reach an 81% accuracy rate following the implementation of the upgrade. (Extremely Intelligent Machine) During the second round of classification research, it was determined that the inability to discern between normal and cancerous pituitary gland images was one of the limiting issues.

f. T. A. Jemimma et al. [7] This diagnostic procedure can precisely find the tumor since it divides the territory inhabited by the tumor in an appropriate manner. The adoption of Jemimma and Vetharaj's innovative Dynamic Angle Projection (DAPP) for isolating brain tumors is a major advancement in the field. Utilizing Dynamic Angle Projection in order to obtain textural data, the Watershed idea successfully splits the tumor zone (DAPP).

g. Nilesh Bhaskarrao Bahadure et al. [8] During the course of our investigation, we divided brain tissues into two groups: those without tumors and those with tumors (white matter, gray matter, cerebrospinal fluid [CSF], and background). Raw MR images were treated to improve their quality and reduce the influence of noise present during data collection. This was done in order to better comprehend the acquired data. Then, our proposed auto-enhance FCM method was utilized to increase the image quality. The threshold concept is utilized during skull stripping to remove extra brain tissue, such as fat and skin, from the patient's head. This procedure is also referred to as a craniotomy. In addition, we provide a metric for comparing the performance of four distinct segmentation methods, including those based on watersheds, FCMs, DCTs, and BWTs. The evaluation of these algorithms is based on how effectively they partition a dataset into discrete pieces. To verify that our segmentation findings were as accurate as possible, we narrowed our candidate pool by comparing the segmentation ratings of each candidate. To increase the accuracy of tumor stage classification, a feature vector is first obtained, then refined, and finally classified with the use of a genetic algorithm. The purpose of this phase is to attain the aforementioned objective. The outcomes of our testing indicate that the proposed technique is effective for facilitating the early diagnosis and precise localisation of brain tumors. The importance of the presented approach, which utilizes MR imaging, for the detection of brain cancers cannot be emphasized. On a collection of magnetic resonance (MR) images, the suggested approach was evaluated, and the findings indicated that it had an accuracy of 92.03 percent, an average dice coefficient index of 93.79 percent, and a segmentation score in the range of 0.82–0.93 percent. Our research findings can be applied to the improvement of clinical decision support systems used by radiologists and other medical professionals for primary screening and diagnosis. Future research will primarily focus on enhancing the precision of the present work and the dice coefficient index. This will primarily be accomplished through the investigation of more robust mechanisms for the vast library of medical images and the classifier's selection approach.

h. S. Arunmozhi et al. [9] Using MRI, the purpose of this study is to identify and assess any schizophrenia symptoms that may be present in brain slices. Within the framework of this study, a segmentation technique was utilized to determine the region of the brain that is most severely impacted by schizophrenia. Experiments done within the scope of this work use two-dimensional MRI slices to demonstrate that the proposed strategy yields superior results.

i. Renuka Devi M N et al. [10] The proposed method for tumor image processing will consist of three steps. After converting RGB photos to grayscale, the pre-processing step consists of applying Gaussian, median, and anisotropic filters to eliminate noise and improve the image quality. Thirdly, both the watershed method and the active contour method are valid solutions for tumor segmentation. In the suggested study, data were compared utilizing both the watershed approach and the active contour method. In addition, it takes advantage of the fact that it is possible to determine the tumor's area and perimeter. Consequently, the method enhances the precision with which brain tumor sizes can be determined in contrast to other algorithms now in use. Comparing the results of the active contour method and the watershed algorithm reveals that the watershed method is superior due to the inaccuracy of the active contour technique in detecting cancerous regions.

j. Kiran et al. [11] Based on magnetic resonance imaging, we describe a computerized radiology system for evaluating brain tumors in this study (MRI). In this study, we utilized the Watershed and PSO algorithms, as well as DWT, PCA, and feature extraction, to construct an SVM model that successfully diagnoses cancer.

k. Leyla Aqhaei [12] This paper presents a hybrid technique for detecting brain tumors in imaging investigations by combining watershed, genetic, and support vector machine techniques. National Cancer Institute conducted the investigation. Using this technique, the images are segmented properly, allowing for a definitive diagnosis of the brain tumor. In order to eliminate noise, the images are therefore pre-processed by applying grayscale and median filters. After the image has been segmented using the watershed method, the genetic traits are analyzed. The SVM algorithm is then implemented in order to learn from the gathered data and provide an accurate diagnosis of brain cancer. In terms of accuracy (95% accuracy), precision (97% accuracy), and memory (89% recall), the examination of the proposed method's capacity to segment and classify images indicates that it outperforms baseline procedures. Comparing the suggested method to the baseline procedures yielded these findings.

l. K. Usman et al. [13] This study's authors present a strategy for the segmentation and classification of brain cancers in multimodality MRI data. The co-registered and skull-stripped data from the 2013 Multi-Institution Critical Comparative Analysis of Imaging of the Brain (MICCAI BraTS) challenge are utilized, and histogram matching is performed with the aid of a highly contrasted reference volume. After the images have been preprocessed, they are evaluated to extract attributes such as intensity, intensity differences, local neighborhood, and wavelet texture. The random forest classifier is used to predict five classes, including background, necrosis, edema, enhancing tumor, and non-enhancing tumor, following integration. These class labels are then utilized to compute three regions hierarchically (complete tumor, active tumor and enhancing tumor). Due to the outcomes of our leave-one-out cross-validation, we were able to enhance the reported Dice overlap from the MICCAI BraTS challenge from 75% to 88% over the total tumor territory, from 75% to 78% throughout the core tumor region, and from 95% across the enhancing tumor region.

m. P. R, et al. [14] In this article, we examine the research conducted on the numerous techniques now utilized to eliminate malignancies from MRI scans of the brain. This section provides both quantitative and qualitative evaluations of the performance of cutting-edge approaches. This article gives context for the several strategies for image segmentation by summarizing recent contributions from a variety of academics. Combinations of Conditional Random Field (CRF) and Fully Convolutional Neural Network (FCNN), as well as CRF with Deep Medic or Ensemble, have been found to be more effective for segmenting brain MRI images of tumors the similarity algorithms (Dice index 84% and Jaccard index 77%).

n. Farzaneh Dehghani et al. [15] This study intends to automate the delineation of brain tumors utilizing FLAIR, T1-weighted, T2-weighted, and T1-weighted contrast-enhanced MR sequences with a deep learning technique. The major objective of the study is to determine which MR sequence alone or combination will result in the highest accuracy the similarity algorithms (Dice index 77% and Jaccard index 64%).

Table 2.1: Summary of Literature Survey.

No.	Researcher	Field of implementation	Results	Year
a	D. et al. [1]	capsule networks	98% success rate at the patient level	2019
b	A. et al. [2]	classification using CNN, CapsNet	using CapsNet on the convolutional layer led to an accuracy of 86.50 percent.	2019
c	Rehman et.al [3]	AlexNet, Transfer learning	using three different studies that have used the convolutional neural network architectures AlexNet, GoogLeNet, and VGGNet to categorize brain cancers.	2019
d	A. et al. [4]	classification using DCNN	generated 91.9% accurate readings.	2019
e	P. et al. [6]	CNN's baseline ELM-based classification model	an 81% accuracy rate following the implementation of the upgrade.	2019
f	T. et al. [7]	Watershed Algorithm based DAPP features	the Watershed idea successfully splits the tumor zone (DAPP).	2018
g	N. et al. [8]	Segmentation and Classification Using Genetic Algorithm	an accuracy of 92.03 percent, an average dice coefficient index of 93.79 percent, and a segmentation score in the range of 0.82–0.93 percent.	2018
h	S. et al. [9]	the purpose of this study is to identify and assess any schizophrenia symptoms that may be present in brain slices	Experiments done within the scope of this work use two-dimensional MRI slices to demonstrate that the proposed strategy yields superior results.	2020

Table 2.1: Summary of Literature Survey 'Tables Continued'.

i	R. et al. [10]	method for tumor image processing will consist of three steps	Consequently, the method enhances the precision with which brain tumor sizes can be determined in contrast to other algorithms now in use	2021
j	K. et al. [11]	Classification system for brain tumor using SVM	construct an SVM model that successfully diagnoses cancer.	2022
k	Leyla [12]	combining watershed, genetic, and support vector machine techniques.	accuracy (95% accuracy), precision (97% accuracy), and memory (89% recall)	2021
l	K. et al. [13]	classification from multi-modality MRI using wavelets and ML	Due to the outcomes of our leave-one-out cross-validation, we were able to enhance the reported Dice overlap from the MICCAI BraTS challenge from 75% to 88% over the total tumor territory, from 75% to 78% throughout the core tumor region, and from 95% across the enhancing tumor region.	2017
m	P. et al. [14]	Fuzzy Neighborhood Learning Approach for 3D MRI Images	similarity algorithms (Dice index 84% and Jaccard index 77%).	2021
n	F. et al. [15]	segmentation from multi MR sequences through a DCNN	similarity algorithms (Dice index 77% and Jaccard index 64%).	2022

2.4 CONCLUSION

With the aid of a median filter, a thorough and effective preprocessing can isolate and remove a considerable amount of an image's artifacts and noise. To solve the problem uncovered by the clinical MRI examination of the tumor, an entirely different technique has been applied. The proposed method, which is based on Watershed segmentation, has been rigorously tested on MRI imaging data, and the findings have been overwhelmingly good. The assessment of the tumor's location and size is performed using a specially created algorithm.

3. MATERIALS AND METHODS

3.1 CHAPTER INTRODUCTION

Digital image processing refers to the alteration of digital images utilizing personal computers. Over the course of the last few decades, its degree of popularity has risen meteorically. It has numerous applications, including in health, the entertainment industry, geology, and even remote sensing. The processing of digital images is necessary to the operation of multimedia systems, a vital aspect of the contemporary information society.

The wide field of digital image processing incorporates both image-specific and signal-processing-general techniques. Consider an image to be a function defined by two continuous parameters, x and y, with the notation f (x, y). It must first be sampled, then converted into a matrix of integers before it can be digitally processed. Quantization is important for the digital representation of numerical data due to the limited precision of computer representation. The processing of digital photos necessitates working with numbers that have a limited range of precision. Image processing can be separated into numerous subfields, with picture editing, image restoration, image analysis, and image compression being the most prevalent. Image enhancement aims to improve an image's ability to convey additional information to a human observer. When a statistical or mathematical explanation of a picture's deterioration is offered, the objective of image restoration is to repair the damaged image using the provided explanation. The numerous methods of image analysis allow for the processing of images with the goal of automatically extracting information from such images. Segmenting a picture, removing its edges, analyzing its textures, and identifying whether an image has motion are examples of image analysis.

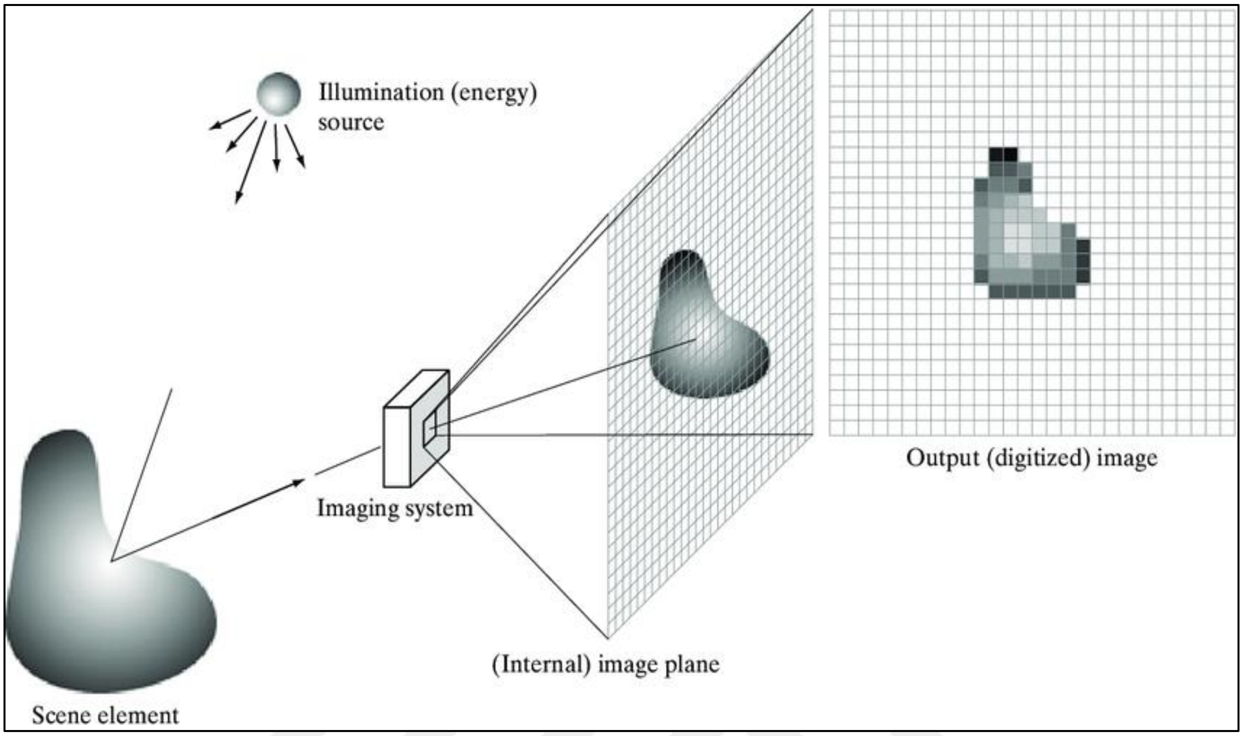

Figure 3.1: Digital image Processing [6].

3.2 DIGITAL IMAGING

Digital imaging is the process of capturing an object's visual features (such as its shape or color) and turning them into a digital representation. This method is sometimes also known as computer image acquisition. It is usual practice to incorporate or include under this umbrella phrase picture processing, storage, printing, and viewing. The capacity to digitally replicate copies of the original subject forever without any image quality loss is a significant benefit of a digital image over an analog image, such as a film photograph. The electromagnetic radiation or other waves that transmit the image's information as they travel through or reflect off objects can be used to categorize different types of digital imaging. Digital imaging is the process of capturing an object's visual features (such as its shape or color) and turning them into a digital representation. This method is sometimes also known as computer image acquisition. The phrase is frequently taken to indicate or comprise such image processing, compression, storage, printing, and display. An important benefit of a digital image over an analog image, such a film photograph, is the capacity to replicate the original object digitally. Medical imaging serves to enlighten patients and lessen the confusion surrounding their diagnoses. The light reflected from the object is to be passed to an imaging system such as analogue to digital convertor (ADC); this convertor applies the sampling and quantization to get the digital image as shown in figure 3.2.

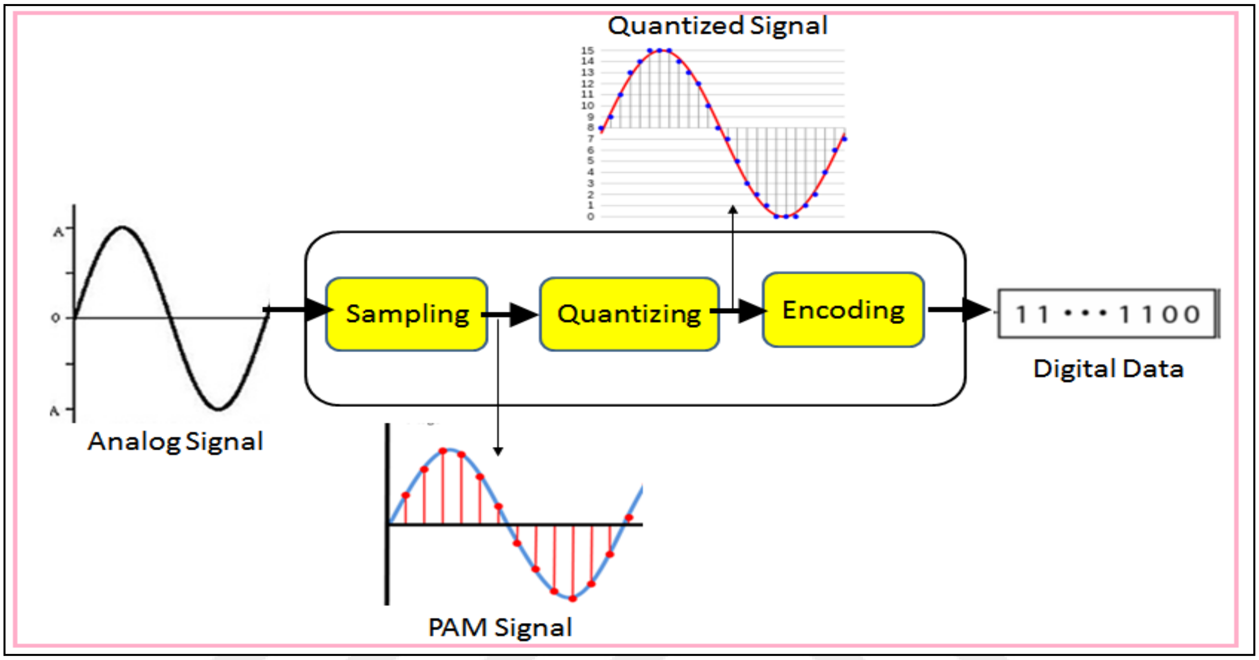

Figure 3.2: Using ADC to form digital image [15].

Health and government organizations are increasingly turning to digital imaging to boost productivity and offer easier access to specific sorts of information. Numerous benefits come with digital photography, such as better dissemination and publication, enhanced access, simpler workflows, and a far lower requirement for physical storage space. Another advantage of digital photography is that digital photos can be transformed into text-searchable files using optical character recognition (OCR) software. When digital images are posted to the Internet and made accessible to users, it paves the way for more efficient communication between businesses and their clients or the public.

Even though digital imaging is becoming more and more widespread, you must keep in mind that it is an investment with potentially extremely significant upfront expenses. Your company or agency should be able to afford digital imaging. Your digitized records must be reliable, complete, and durable for as long as your approved records retention schedules call for to guarantee that they are fully admissible in court.

3.2.1 MRI

Since its initial demonstration in 1973, magnetic resonance imaging, or MRI, has developed into a sophisticated analytical modality that is widely utilized in both clinical practice and research as a diagnostic tool. Comparing it to diagnostic methods like X-ray imaging reveals various advantages. It doesn't involve any radiation and is non-invasive. There are not many drawbacks. People with pacemakers cannot be imaged, though, as MRI uses radio waves and strong magnetic fields. Other types of metallic implants inside the body may also prevent imaging. The instruments also require a lot of room that has been particularly developed and are still quite pricey and hefty. Typically, they conduct business out of their own property. The magnetic resonance imaging (commonly known as MRI) scanner is a cutting-edge diagnostic tool that can provide insight into an organism's inner workings. Although an animal or a human body is typically the subject, MRI is also employed in the sector for more technical uses. The biggest benefit of MRI is its ability to provide three-dimensional images of the thing being studied without endangering it and without emitting any ionizing radiation.

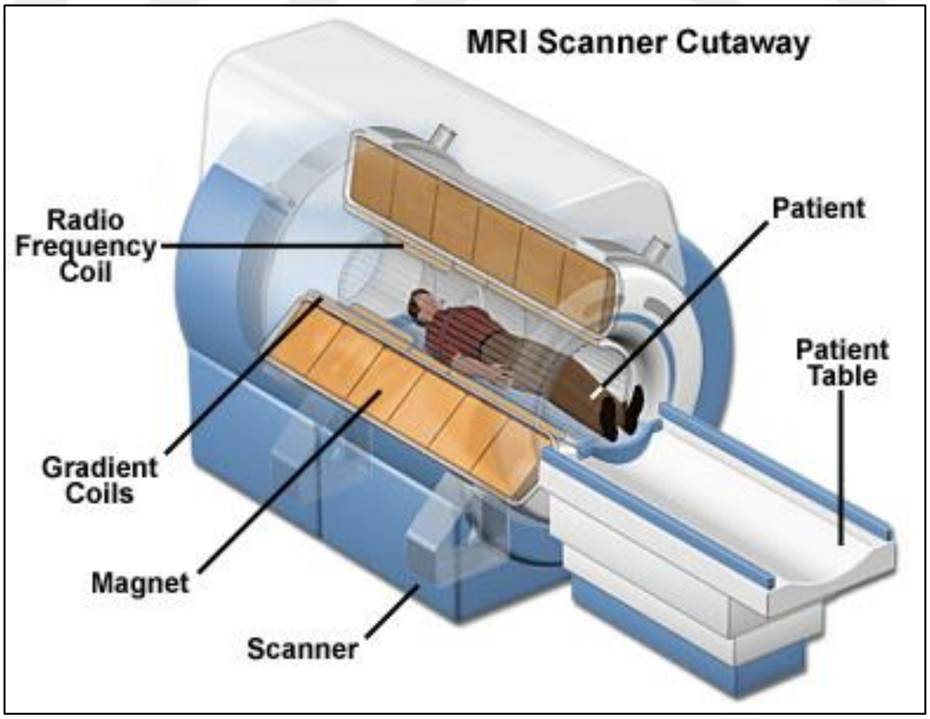

Figure 3.3: Clarification MRI (Magnetic Resonance Imaging) [46].

MRI's Characteristics Brain tumors appear in a number of forms, from primary to metastatic, and malignancy grades; feature extraction from MRIs can assist medical personnel in detecting patterns that can be used by classification algorithms to differentiate between distinct illnesses. Software-based digital image analysis is more accurate and efficient than untrained human analysis. Those observers can draw more accurate conclusions to make a diagnosis of a brain tumor [14].

In different stages of treatment, in addition to determining whether a brain tumor is malignant, an MRI can reveal information about the patient's prognosis. Images can occasionally be spatially diverse. Additionally, there are overlaps with normal tissues in some photos, mainly in the invading area. Glioma tumors exhibit several mixed characteristics, such as simultaneously displaying both high- and low-grade characteristics. The surgical biopsy is necessary for the classification of brain tumors; however, this classification frequently relies on the removal of tissue from the biopsy, which can be quite dangerous [15].

Its objective is to create an automated tool that can aid in the examination of images of brain tumors. This instrument will be capable of determining the grade of the glioma and distinguishing between various forms of tissue, including primary neoplasms (gliomas) and secondary neoplasms. This will permit the analysis to proceed faster (metastases). These concerns are crucial clinical considerations while choosing the initial treatment plan as well as an evolving one. Typically, conventional MRI is less effective at providing answers [15].

In instances where the neoplasm is heterogeneous and, as a result, it is not possible to sample the neoplasm efficiently using a localized needle biopsy, WE avoid using invasive procedures, including biopsy, especially when the risks outweigh the benefits, and (iii) anticipate the diagnosis using validated automated tools. Future differentiation may be more reliable as a result of automated technologies that have proven their accuracy (histological examination often takes a long period of time). The investigation in question utilized both spectroscopic and perfusion MRI techniques, focusing on four unique areas within the tumor and the surrounding tissue. [16] Numerous studies have employed MRI spectroscopy to classify brain tumors and distinguish between malignant and benign disease types.

Several further studies, however, have paired the Apparent Diffusion Coefficient (ADC) with the Cerebral Blood Volume (CBV), which is used to differentiate primary neoplasms from lymphomas and abscesses. The Apparent Diffusion Coefficient, often known as ADC, is determined by the diffusion measurement in peritumoral edema [17-15]. This enables the ADC to distinguish between cancerous and benign tumors.

It is not easy to separate a brain tumor from the surrounding tissues due to the following factors:

a. The disorganized brain tissue surrounding the tumor mass as a result of tumor growth, which produces a variety of gray colors.
b. Edema, who mainly manifests as white margins surrounding the tumor and may contain swelling cells around the tumor and will appear as white matter in the MRI, can sometimes cause swelling and infiltration of brain tissues.
c. The progressively developing mutation between the tumor, surrounding brain tissue, and edema results in hazy boundary detection [15].
d. Flair in MR imaging that standard appears white in imaging for delineating any tumor in the brain, as well as the blood vessels appearing as a brilliant regains also for that the information that acquired from extraction is not always as clear as desired and it is.

almost not possible to segment small area from MRI by thresholding image intensity [15].

3.2.2 CT Scans

The development of X-ray computed tomography (CT) was influenced by a number of significant scientific advances, including the discovery of X-rays, an increase in processing power, and the advent of digital X-ray data collection technology (CT). Computed tomography (CT), which reconstructs anatomical images of internal structures using X-ray attenuation coefficients (roughly comparable tissue density) for almost all body parts, can replace conventional X-ray imaging. CT is an alternative to traditional X-ray imaging, often known as general radiography. As a result, computed tomography (CT) imaging can be used to diagnose a wider range of conditions than standard X-ray imaging. Clinical applications consist of parameters for image capture, CT angiography, image processing, and vertex placement. Clinical applications also include integrated imaging modalities such as positron emission tomography (PET) and single photon emission computed tomography (SPE-CT). This process is referred to by the acronym "single photon emission computed tomography". In the disciplines of radiation and diagnostics, a deeper understanding of CT features, such as those that improve image quality and exposure dosage optimization, can lead to more effective and precise patient treatment. This can be accomplished by a greater understanding of CT characteristics. The development of CT scans was considerably facilitated by the discovery of X-ray radiation, a crucial intermediate step. On November 8, 1895, German physicist Wilhelm Conrad Roentgen conducted the first tests on a cathode tube (also known as a Crookes tube) [25]. This light is capable of fluorescence, can pass through opaque materials, and can sensitize film. This sort of radiation was known as X-ray radiation by Röentgen. Three-dimensional objects are penetrated by irradiation X-rays. Images in two dimensions are created on films or detectors by X-rays that pass-through objects. Radiography is the general term used to describe this. Due to overlap, it is difficult to distinguish between tissues with small absorption coefficients, and scattering X-rays have a negative impact on the generation of images. Conventionally, two-dimensional CT images are made to look as though the patient is standing at the patient's feet and looking up at the image. Given that the patient's right side is the image's left side and vice versa, as well as the image's anterior being the patient's posterior, this indicates that the image's right side is the patient's right side and vice versa. It should not be surprising that doctors lean to the left when standing in front of patients, given this is their natural posture [24-26]. The diagram shows CT scanner working principal Figure 3.4.

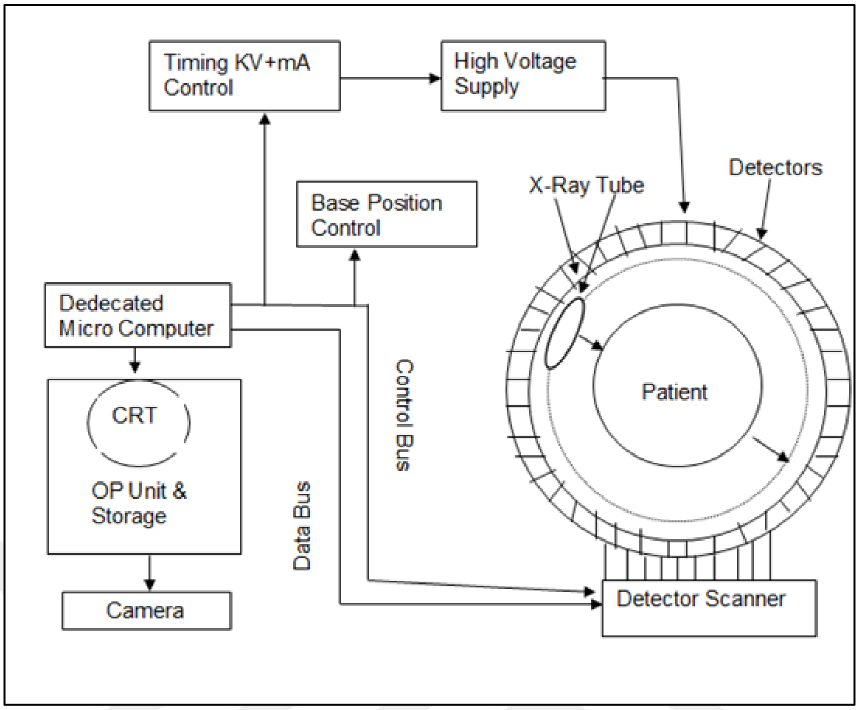

Figure 3.4: block diagram of CT Scanner [46].

3.2.3 X-RAYS

X-ray devices produce invisible beams of electromagnetic energy that can be used to capture images of inside organs, bones, and tissues on film or digitally. Only two of the many applications of standard X-rays are the diagnosis of cancer and the examination of bone deterioration. X-raying is an imaging technique that uses an external radiation source to produce images of the body, its organs, and other interior structures for diagnostic reasons. X-rays that have travelled through human tissue and settled on precisely treated plates (similar to camera film) or digital media produce a "negative" image of the internal architecture of the body. When X-rays are permitted to travel through human tissue, this image is produced (the more solid a structure is, the whiter it appears on the film). When a person is X-rayed, their body simultaneously allows varying levels of radiation to travel through its various components. Because soft tissues such as blood, skin, fat, and muscle are able to absorb the majority of X-ray energy, they will appear dark gray on an X-ray photograph or digital image. Denser tissue, such as bone or a tumor, blocks more X-rays, causing that tissue to appear white on the image. On an X-ray, a fractured bone might look as a dark line running through a piece of bone that is otherwise white. X-ray technology is utilized in numerous diagnostic procedures, including arteriograms, computed tomography (CT) scans, and fluoroscopy. There is a possibility that each X-ray procedure follows to a slightly different set of criteria, and this differs from institution to institution.

a. Lead aprons (shields) may be used to shield body portions from the X-rays that are not being photographed.
b. The imaging target will be the focal point of the X-ray beam.
c. To avoid blurry images, the patient must maintain extreme stillness.

For instance, a chest X-ray may take images from both the frontal and profile views simultaneously.

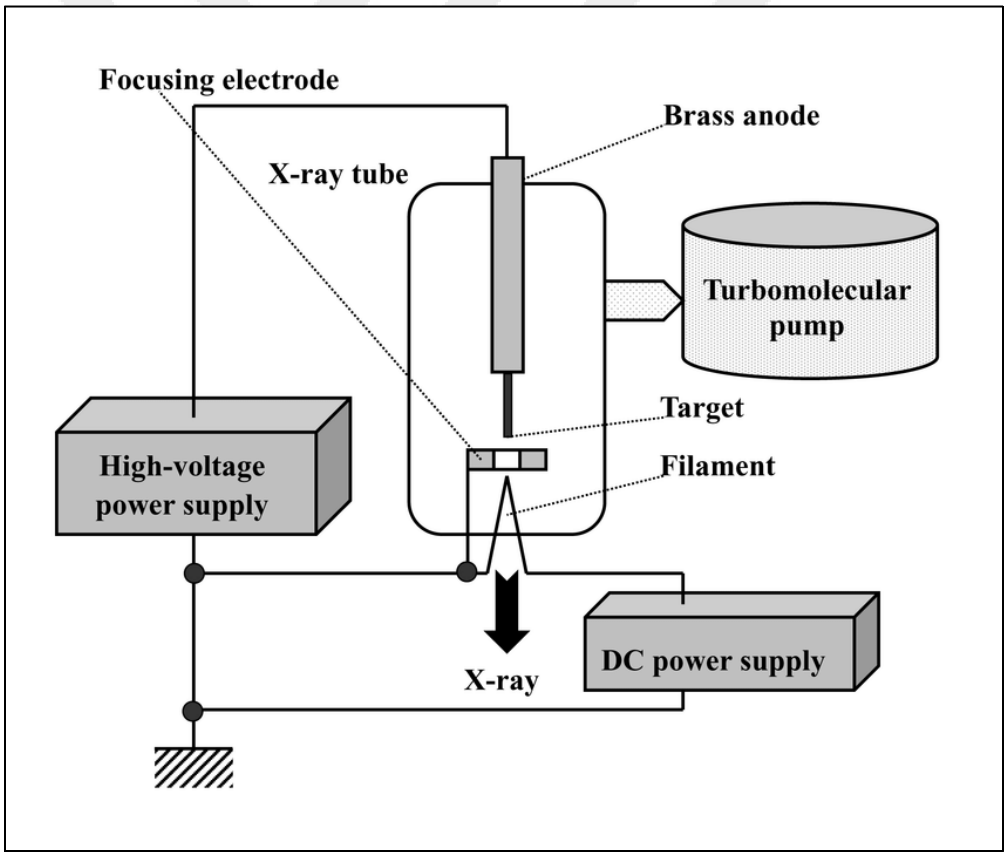

Figure 3.5: Block diagram of a characteristic x-ray generator [47].

3.3 IMAGE PROCESSING

The term "image processing" refers to a range of techniques that can be applied to an image to enhance it or extract pertinent data. One can apply these approaches to an image in a variety of ways. The "input" for this sort of signal processing is a single image, and the "output" might either be an entirely new image or a subset of the qualities contained in the "source" image. The domain of image processing is one of the most rapidly increasing sectors of technology at the present time. Engineering and computer science devote a substantial number of resources to the exploration of this issue. Image processing can be split down into the following three different steps:

i. The first step is to purchase the image, followed by its importation.
ii. The process of inspecting and modifying an image.
iii. Outputs may be a changed image or a report outlining the analysis's findings.

Both analog processing and digital processing are viable technologies for picture processing. Using analog image processing, it is possible to reproduce images in non-digital formats such as prints and images. When applying these visual techniques, image analysts employ several interpretational fundamentals. Computer-based digital image alteration is made possible with the use of digital image processing tools. When employing digital technique, all forms of data must go through three general phases: pre-processing, augmentation, and presentation; and information extraction.

3.3.1 Image Filtering

When it is necessary to improve or recover data from inside an image, image filters are often employed. These filters act by reducing or eliminating the level of visual noise while mostly preserving the image's underlying structures. The great majority of computer vision and computer graphics applications use image filtering to decrease the impact of noise and restore fundamental visual structures. Typically, simple explicit linear translation-invariant (LTI) filters are used for edge detection, feature extraction, blurring, and sharpening images. These filters include the Gaussian, Laplacian, and Sobel models [27].

a. Median Filter: The median filter is a technique for nonlinear signal processing that is based on statistical analysis. When processing a digital image or sequence, the image's or sequence's surroundings' median value is substituted for the noisy original (mask). The mask's pixels are ordered according to their darkness, and the value corresponding to the group's median darkness is retained in place of the noisy value. Background noise-suppressing characteristics of the median filter Given that the median filter for a noisy image is a nonlinear filter, it can be challenging to analyze it analytically. The median variance of filtering noise for an image with a normal distribution and zero mean noise is

$$\sigma_{med}^2 = \frac{1}{4nf^2(n)^-} \approx \frac{\sigma_i^2}{n+\frac{\pi}{2}-1} \cdot \frac{\pi}{2\cdot} \tag{3.1}$$

where σ_{med}^2 where n is the size of the median filtering mask and are constants. $f(n)^-$ depending on how much background noise there is. The standard deviation of the noise is the same for the filtering operation itself

$$\sigma_0^2 = \frac{1}{n}\sigma_i^2 \tag{3.2}$$

Comparing of (3.1) and (3.2), The outcomes of using a median filter depend on two variables: the size of the mask and the distribution of the noise. The median filter is more successful than the average filter when it comes to reducing random noise. However, it is especially beneficial for minimizing impulse noise, which arises when narrow pulses are spaced further apart and their width is less than n/2. It is anticipated that combining the median filtering algorithm with the average filtering algorithm to make adaptive adjustments to the mask based on the noise density will increase its performance.

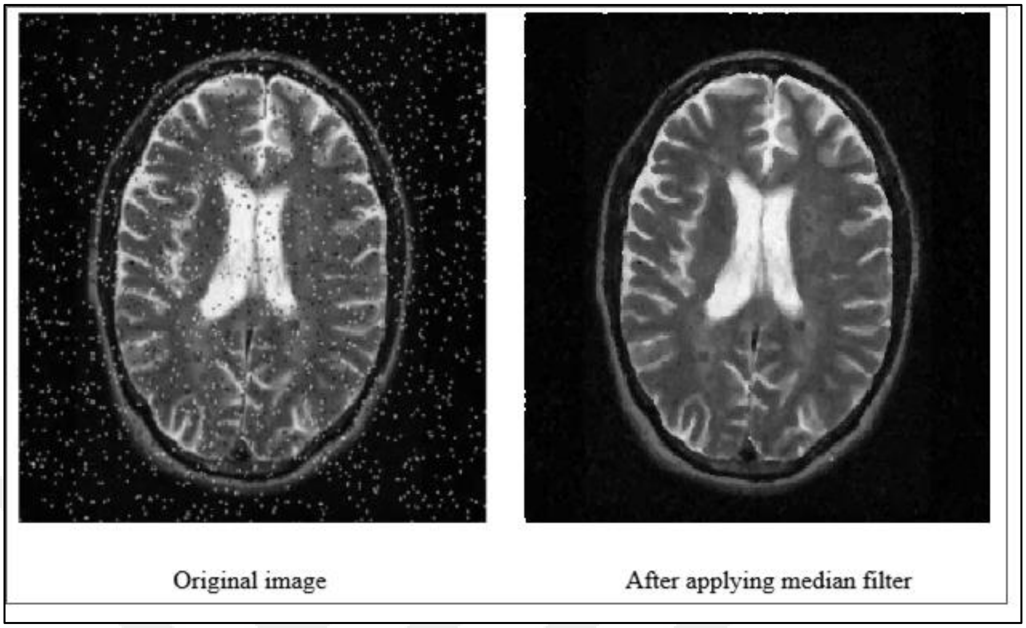

Figure 3.6: The difference appears before and after applying median filter [28].

b. Mean Filter: Smoothing an image is any procedure that changes one image into another in order to remove the abrupt grayscale transitions that occur between adjacent pixels. Smoothing can be achieved through the use of an averaging mask, which involves replacing the central pixel with an image whose gray level equals the average of the surrounding pixels. Due to the fact that all mask coefficients are positive and add up to one, the original level of brightness is retained despite the blurring of the image. Using the mean filter, smoothing can be achieved with moderate ease and decent results. Because the mask must be repeatedly shifted across the image to encompass each pixel, mean filtering is commonly seen as a convolutional operation. The idea of gradually simplifying an image's elements is simply understood by the reader. The simplest method entails simultaneously substituting the value at each image point with the mean of the values contained within an aperture surrounding that point. When this procedure is repeated numerous times, the image loses a portion of its intricacy. The results of such modification rely on the aperture's dimensions and geometry. With smaller apertures and more iterations, the limiting process becomes increasingly apparent, and this awareness can be used to escape dependence on the limiting process. When the number of iterations is decreased to an insignificant amount, the aperture size is dropped to zero and the time parameter is substituted. If we limit ourselves to differential image measurements, we can demonstrate that the effect of intestinal alterations can always be described by a partial differential equation (PDE). The use of PDE systems in image processing is becoming increasingly prevalent.

$$\frac{1}{9}\begin{bmatrix}1 & 1 & 1 & 1\\ 1 & 1 & 1 & 1\\ 1 & 1 & 1 & 1\\ 1 & 1 & 1 & 1\end{bmatrix} \qquad \frac{1}{n^2}\begin{bmatrix}1 & 1 & \cdots & 1\\ 1 & 1 & \cdots & 1\\ \vdots & \vdots & \ddots & \vdots\\ 1 & 1 & \cdots & 1\end{bmatrix}$$

(A) (B)

Figure 3.7: The mean filter (a) 3 × 3; (b) n × n.

c. Fuzzy Logic Filtering: Mathematical morphology is a technique utilized in grayscale image processing. The domains of fuzzy logic and fuzzy set theory offer a variety of potential solutions. It is a word referring to the variety of techniques used to evaluate and portray digital photos. Picture segmentations and features are represented as fuzzy sets in both the coding and defuzzification of fuzzy data (images) [28], with the former depending on the latter and both being influenced by the context. After completing these two procedures, the grayscale plane of the digital image data may be translated into the membership plane. This is the plane on which the fuzzy effects can be applied. Because of this, a fuzzy logic approach to the analysis of images can now be developed [28]. The editing of digital images to create a fuzzy effect typically involves three phases. A fuzzy check is performed on an image, its membership values are modified, and then the fuzzy check is repeated if necessary [28, 29].

The advantages of using fuzzy logic for digital images are:

a. The special features requirement of pattern description that has been used in various algorithms is being overcome by the fuzzy logic.
b. It allows the simple inclusion of human's intention in process of formulation algorithm goals.
c. 3- It gives very good result even if the image blurred or in no good quality.
d. The grayness ambiguity in the gray level image manages easily [29].

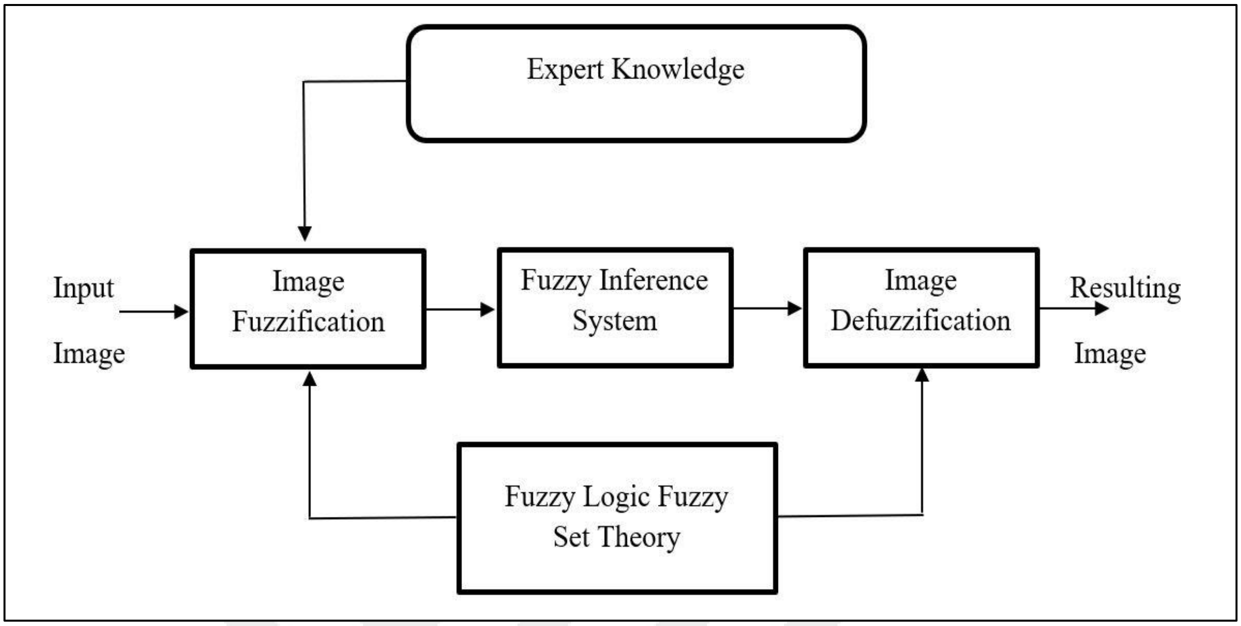

Figure 3.8: The General Structure of Fuzzy Processing.

3.3.2 Histogram Equalization

Image enhancement is a crucial skill for both human and machine vision. This technique is widely employed in the field of medical imaging, as well as speech recognition and the creation of textures, amongst a multitude of other fields. Numerous brainstorming sessions have been held in an effort to develop these strategies. The bulk of these techniques rely on linear or nonlinear gray-level transformation functions, although some need a more complex examination of various image characteristics such as edges and associated components. Using a technique known as hexagonal histogram equalization, image contrast is frequently enhanced (HE). It has become the industry standard due to its user-friendliness and excellent performance on virtually all picture types. HE remaps the gray levels of the image according on the probability distribution of the gray levels in the input image in order to complete the task it was assigned. This technique is widely used to enhance the overall contrast of a number of images, especially when the image is represented by a restricted number of intensity values. This modification allows the entire intensity range to be utilized uniformly across the histogram, resulting in a more uniform distribution of intensities. As a result, areas with little local contrast have the opportunity to raise their degrees of distinction. This is achieved through the application of histogram equalization, which effectively disperses the densely packed intensity values required to reduce visual contrast. This strategy works particularly well with images that contain both bright and dark features. This method can enhance the visibility of bone structure in x-ray images, for instance, as well as the clarity of underexposed or overexposed images. This method's key benefit is that it is a straightforward procedure that can be quickly modified to handle any particular input image and any operator that can be reversed. If the histogram equalization function is therefore known, it is theoretically possible to recover the original histogram. The calculation needs minimal computational effort from the user. The downside of this technique is that it lacks any form of vision. At the expense of the signal's integrity, the background noise may become more distinct. Histogram equalization is a technique that may be applied to an image to increase its contrast by adjusting the intensity levels. Assume that a specific image, represented by, exists as a matrix of the type mr by mc and that the intensities of its pixels fall within the interval [0, L-1]. The letter L represents the maximum number of intensities that can be used, which is usually 256. For convenience, we will refer to the histogram of with bins for each intensity level as p. [30]. So

$$p_n = \frac{\text{no. pixels with intensity } n}{\text{total no. pixels}} \; N = 0, 1, \ldots, L-1 \tag{3.3}$$

The histogram equalized image g will be defined by

$$g_{i,j} = \text{floor}\left((L-1)\sum_{n=0}^{f_{i,j}} p_n\right) \tag{3.4}$$

where floor ($f_{\mathrm{I,j}}$) rounds down to the nearest integer [30].

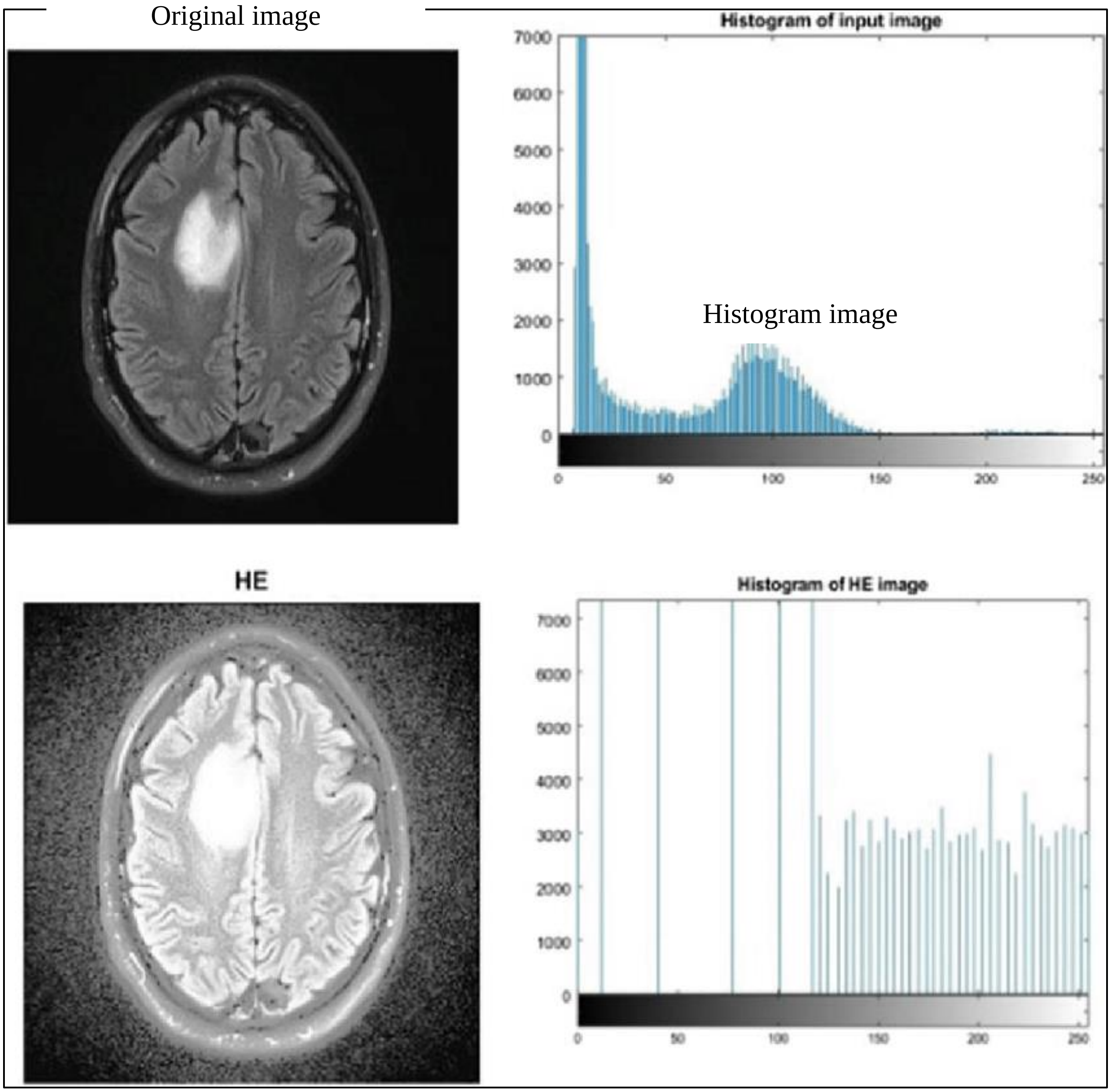

Figure 3.9: Histogram equalization applied to low contrast image [30].

3.3.3 Segmentation

Picture segmentation is the process of breaking a digital photograph into smaller portions, often referred to as "image regions" or "image objects." This procedure is known in the field as "image segmentation" (sets of pixels). [31, 32] The process of segmentation simplifies and modifies the representation of an image to make it more accessible and suitable for analysis. This is achieved by disassembling the image into its constituent pieces. Using image segmentation, it is possible to identify the objects and boundaries (lines, curves, etc.) present inside an image. To segment an image, you must first determine the unique qualities of each pixel and then label them based on your observations. When two or more pixels inside a picture share the same label, we refer to these pixels as constituting a segment. It has been said that a picture is worth a thousand words since it is easier to understand than a lengthy explanation. One of the most advantageous applications of digital image technology is the ability to analyze an image and extract information from it without altering the image itself. This is one of the most important uses of digital image technology. [33] Research in the fields of pattern recognition, image analysis, and related picture disciplines has been a major focus of computer science and computer engineering for the past three decades. [33] Included in these fields are pattern recognition, image analysis, and other image-related sciences. In the actual world, these spheres have applications in astronomy, the medical industry, and the military, among others. It has been discovered [34] that image segmentation algorithms may be divided into three basic categories: boundary-based, region-based, and hybrid-based. [35] The first way of image segmentation is called the discontinuity approach, and it entails selecting points, lines, and edges that have recently undergone significant changes in their local attributes. Thus, we are able to pinpoint the precise locations where each of the various zones begin and end. Utilizing shared characteristics among the elements of geographically dense data, the second segmentation approach delivers a result. These shared characteristics include texture, intensity, and hue. Combining the region-based and boundary-based segmentation approaches as in the third technique Figure. 3.10.

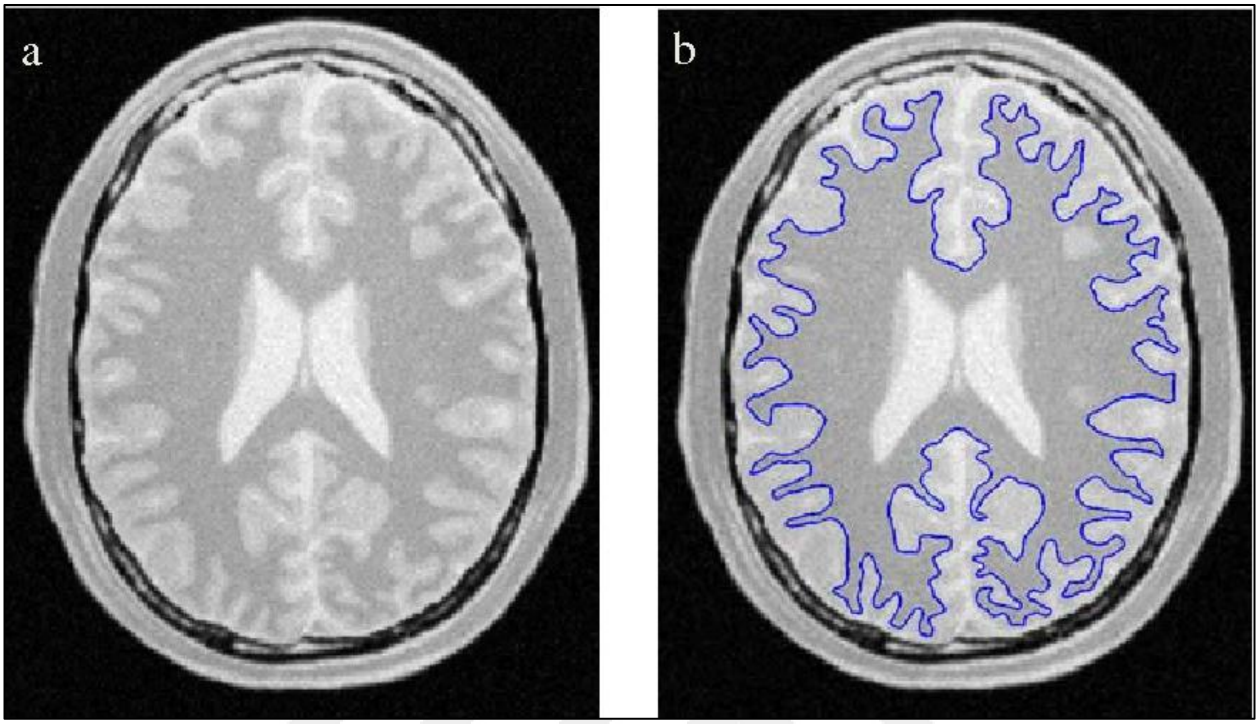

Figure 3.10: Example of medical image segmentation where (a) MRI Image (b) segmented MRI Image [33].

Present segmentation techniques often only distinguish between objects and backgrounds, require prior data knowledge, and require user-specified input parameters. This can result in under- or over-segmentation as well as environmental control loss. Consequently, there is the potential for enhanced photo classification through the strengthening of existing algorithms. Despite the huge amount of published material about images segmentation and the great diversity of methodologies employed, segmentation can be achieved through a vast array of categories. Thresholding, edge-based segmentation, region-based segmentation, and energy-based segmentation are some examples of these categories.

a. K-means Segmentation: Clustering is one of the most efficient techniques that may be used in conjunction with other methods, and it is also one of the simplest. Other choices in this context include the K-means, Fuzzy C-means, mountain, and subtractive clustering techniques. k-means is one of numerous accessible clustering algorithms, and it is one of the most popular. This approach can be implemented more rapidly and with fewer processing resources than hierarchical clustering. Additionally, it can be used to a vast array of distinct variables.

However, the results are widely different according on the number of clusters employed. Consequently, it is important to conduct an appropriate cluster initialization with k equal to 2. The k-value of the centroid must be reset to its starting value of zero. If the initial centroid's value differed from the current value, a new cluster would be established. Consequently, selecting a dependable initial centroid is essential. The K-Means method permits the classification of things according to their degree of similarity. To put it another way, clustering algorithms are unsupervised, meaning they cannot utilize data that has been tagged. After assessing the degree of similarity between the various data sets, one can categorize or cluster the data into more relevant categories. Within the same group, the degree of similarity between data points is at its maximum, whereas it is at its lowest when comparing data from different groups. Commonly used for data clustering, the K-means method is highly prevalent. The effectiveness of the K-means method of clustering has been established:

i. Choose the cluster size, denoted by the letter k, that you want to use.
ii. Randomize the placement of each data point within each of the k clusters.
iii. It is essential to identify the cluster cores.
iv. It is required to estimate the distance between each cluster's individual data points as well as the nodes that connect the clusters.
v. Create new clusters from the data points according to their distances from the existing clusters.
vi. Determine where the new center of the cluster is.
vii. Repeat steps 4, 5, and 6 until the data points no longer influence the clusters or until the maximum number of repeats is reached.

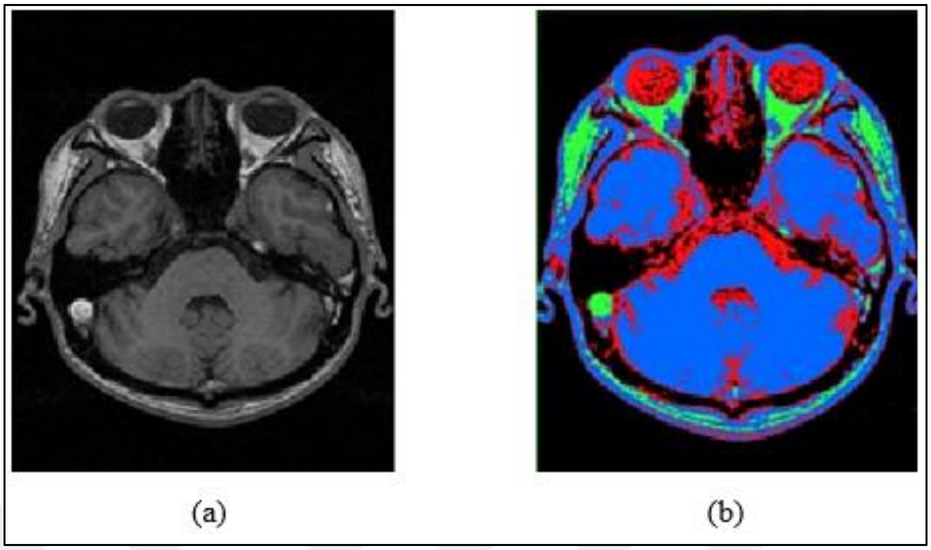

Figure 3.11: Segment image Using K-means: (a) MRI Image (b) After applying the K-means clustered [34].

b. Semantic Segmentation: The assignment of a semantic class name to each pixel within an image is one of the key issues confronted by computer vision researchers. It has been the focus of considerable and active study in a number of recent publications, as it is necessary for such a wide range of demanding and crucial applications, including autonomous driving, augmented reality, and image editing. This is due to the fact that it has been the subject of numerous publications in recent years. Particularly notable are cutting-edge semantic segmentation approaches [35]. The diagrams below illustrate two distinct context aggregation procedures based on paying close attention [36].

i. The non-local module builds a dense attention map with H × W weights (such as blue) given to each unique location (in green) [37].

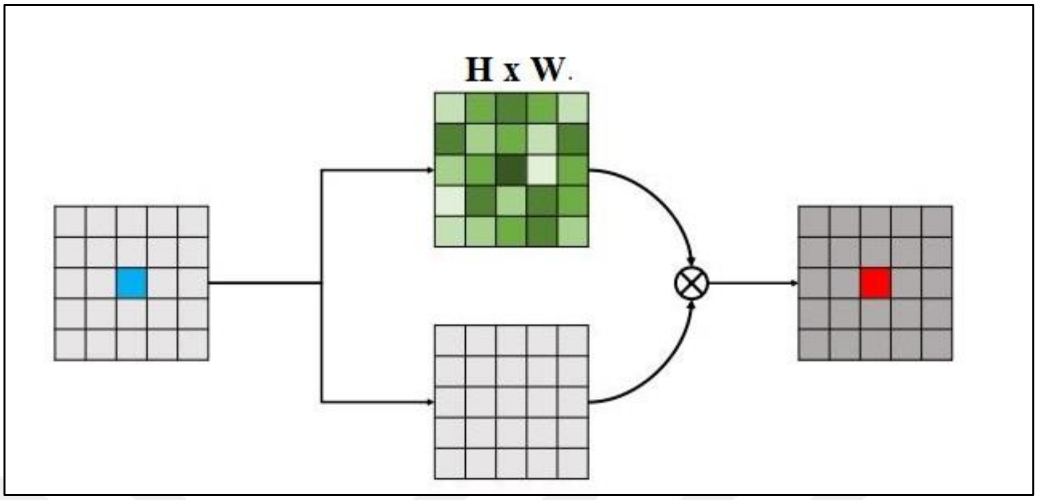

Figure 3.12: non-local block [37].

ii. The sparse attention map produced by the crisscross at tension module has just H + W - 1 weights per point (such as blue).

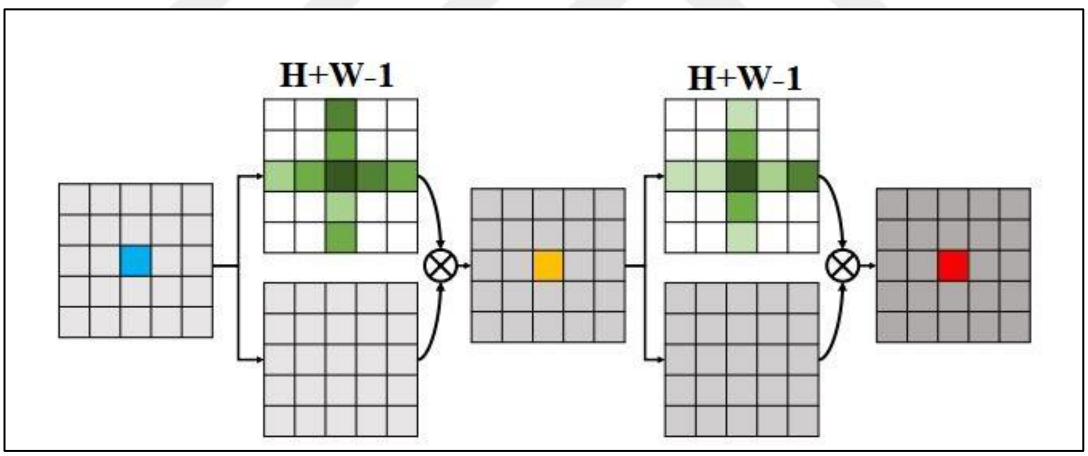

Figure 3.13: Criss-Cross Attention block [37].

Following the iterative procedure, every pixel (such as red) The feature maps of the final result are able to generalize information gathered from any input pixel. In the interest of achieving greater openness, residual links will not be considered.

c. FCM segmentation: In pattern recognition and data mining, the fuzzy clustering method is an example of an unsupervised strategy that has proven to be effective (FCM). Nonetheless, when it comes to the segmentation of medical images, FCM has two significant shortcomings:

a. FCM is unable to achieve the desired results despite its heavy emphasis on color information since it does not take spatial considerations into account.
b. Due to its iterative nature, the objective function minimization employed by FCM is inefficient and cannot match the real-time requirements imposed on image processing.

Implementing algorithms such as the FCM can aid in resolving either of these issues. Because the desired objective function is more complex, each iteration will run faster, saving time throughout the process. Because some better algorithms require more than an hour to complete a single iteration [38], they cannot be used to segment medical images. In order to resolve this issue, a two-stage FCM algorithm with enhanced functionality has been created. First, the image's histogram will be utilized to extract various intervals; secondly, an enhanced version of the fast-convolutional method (FCM) will be employed for segmentation in the second stage. The cluster centroids can be determined using the image's histogram's extracted multiple intervals. Not only is the FCM algorithm vital to the processes of pattern recognition and data mining, but it also has applications in target tracking and picture processing. The key notion underlying FCM-based image segmentation schemas is the transition to a more gentle segmentation technique that preserves as much of the original data as is practically possible. The traditional FCM is distinguished by its emphasis on iteratively decreasing the value of the objective function, which may be expressed mathematically as follows:

$$J(U,V) = \sum_{i=1}^{C} \sum_{j=1}^{n} u_{ij}^{m} d_{ij}^{2} \tag{3.5}$$

where C is the maximum number of clusters that may be utilized, n is the no. pixels in the given image, $m \geq 1$ Changes can be made to modify the degree of ambiguity in the clustering's final results, U_{ij} is the membership of pixel x_j to the ith cluster such that $\sum_{i=1}^{C} u_{ij} = 1$, and $d_{ij} = \| xj - vi \|$ represents the average distance between cluster centers or the average distance in pixels, whichever is greater, $v_i = \sum_{j=1}^{n} u_{ij}^{m} x_j / \sum_{j=1}^{n} u_{ij}^{m}$ is the ith cluster centroid. Membership Prior to producing U_{ij}, which is useful for image segmentation, the objective function must be minimized. Because FCM does not utilize spatial information, FCM-S [7] was developed as a solution to this issue. According to this proposal, a pixel's label would depend on its neighbors' labels. Specifically, FCM-S modifies its objective function so that it now reads

$$J(U,V) = \sum_{i=1}^{C} \sum_{j=1}^{n} u_{ij}^m d_{ij}^2 + \frac{\alpha}{N_R} \sum_{i=1}^{C} \sum_{j=1}^{n} u_{ij}^m \sum_{x_k \in N_j} d_{ik}^2 \tag{3.6}$$

where is *a* parameter that represents the influence of proximity on preference, and are constants. The remaining symbols are identical to those used in the frequency-counting method, and Nj is the set of adjacent pixels to the ith pixel. NR is the total number of pixels surrounding the ith pixel (FCM). Using the process of reduction, formal formulations of the functions U_{ij} and V_i of FCM-S are also attainable Fig. (3.4). FCM-S is developed in the same manner as FCM, but it is less sensitive to interference from environmental noise because it additionally considers its neighbors.

This suggests that the predetermined number of iterations in FCM S is frequently more than the number of iterations in FCM. To obtain greater levels of productivity,

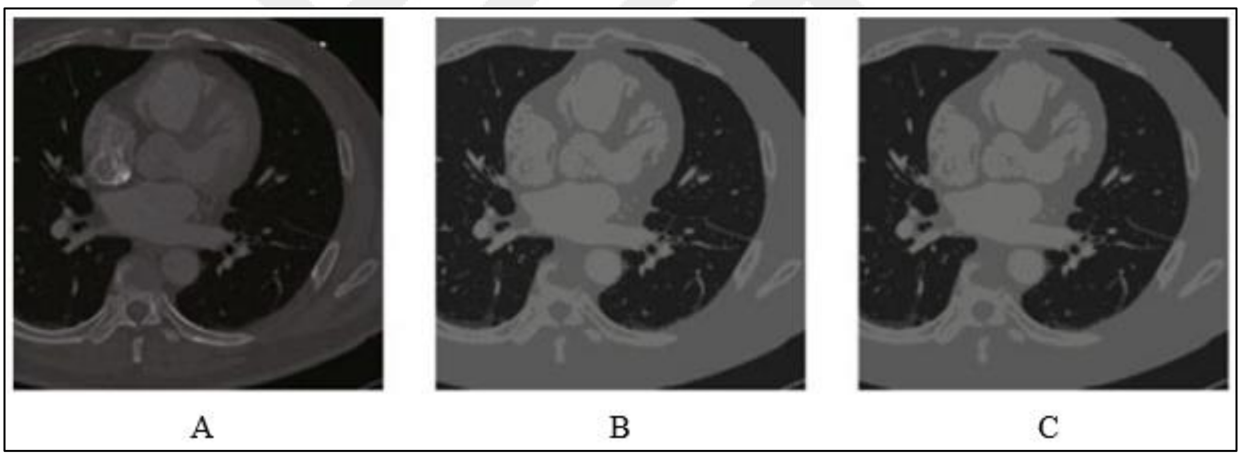

Figure 3.14: Comparison of FCM and FCM-S (C = 4). (a) A medical image. (b) result of FCM. (c) result of FCM-S [7].

d. Watershed Algorithm: The watershed method is one of the most well-known and effective picture segmentation techniques. Due to its capacity to separate images into distinct zones, it is incredibly useful in medical image processing. The watershed algorithm is a segmentation technique that is inspired by topology and mathematical morphology. [38] It is able to detect image borders down to a single pixel and construct exact blocked zones. Additionally, it can swiftly calculate results [39]. On the other side, it is incredibly sensitive to image noise and tiny texture features. Due to the excessively fine granularity, the image may be easily separated into its constituent pieces; yet the lack of contrast renders certain crucial boundary lines unstable. over segmentation is a more serious problem. To address the problem of excessive segmentation, a large number of industry experts and academics have proposed a range of algorithmic solutions for watershed segmentation. These enhancements can be categorized into two primary groups for convenience. Using techniques such as gradient images, noise removal, and target area marking to pre-process the original image before to watershed segmentation is one way to limit the amount of segmentation errors. [40-42].

To perform preliminary segmentation on low-resolution images, the proposed method employs an algorithm known as a watershed. The following strategies are utilized to divide watersheds using markers:

i. The output of this phase is then used as an input for the marker-controlled watershed segmentation, which follows the computation of the picture gradient.
ii. Determine the locations of landmarks in the background These are the pixel clusters located within each unique object.
iii. Calculating the background markers requires effort. These are merely a random assortment of useless, jumbled pixels.
iv. It is necessary to perform calculations using a watershed transform. Initially, the output contours from marker-controlled watershed segmentation will serve as the foundation for IGVF's active contours.

3.3.4 Edge Detection

Edge detection is the process of identifying edges inside an image. Large variations in the luminance of an image's individual pixels can be used to calculate the distances between the image's various components. The great majority of edge detection methods employ a two-dimensional filter that is specifically designed to recognize huge gradients. In the literature, numerous edge detection operators have been identified, each of which is tuned to identify a specific type of edge. Due to the fact that both the noise and the edges transmit high frequency information, it might be challenging to recognize edges in images that contain noise. It is possible that the edges will become less apparent if the noise is eliminated. Edge detection is a critical first step in the segmentation process for medical images. This step is crucial for accurately recognizing human organs such as the skull and tissue. Ultimately, the effectiveness of the edge detection technique will determine the success or failure of the image processing. Historically, edge detection was performed using algorithms and techniques such as the Sobel algorithm, the Prewitt algorithm, and the Laplacian of the Gaussian operator. Theoretically, each of these techniques belongs to the class of high-pass filtering, and as such, they are not suitable for noise suppression. Due to the presence of both noise and edges in the diagnostic photo high frequency band, edge detection is essential.

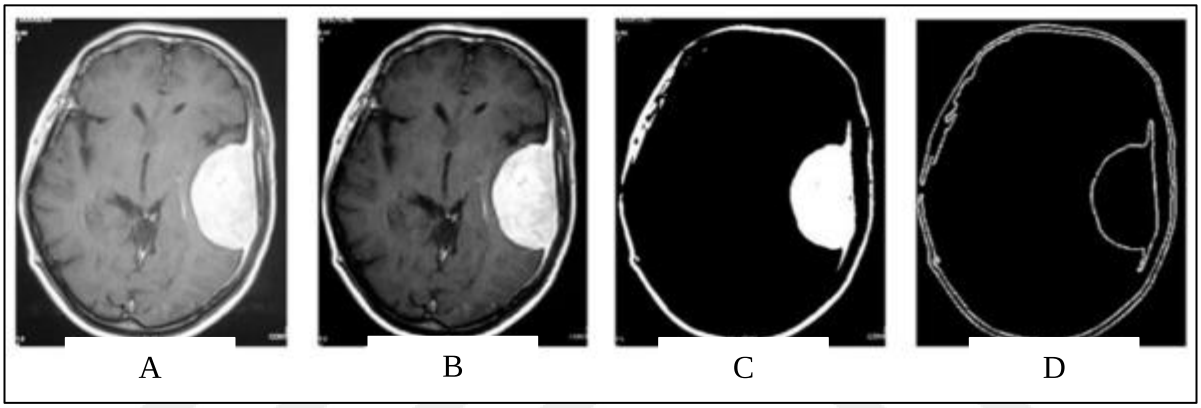

Figure 3.15: (a) Image, (b) Enhanced (c) After applying FCM (d) edge map detection [22].

3.4 BRAIN TUMORS

A brain tumor is a cluster of cancerous cells that have spread throughout the brain. Numerous unique subtypes of brain tumors exist. Malignant brain tumors are quite uncommon compared to benign brain tumors, which account for the great majority of all occurrences of brain cancer (malignant). Primary brain tumors, as opposed to secondary brain tumors, arise from cells that are already present in the brain, whereas secondary brain tumors result from the spread of cancer cells from another organ or part of the body to the brain. The rate at which a brain tumor grows can vary significantly from one patient to the next. The impact of a brain tumor on a patient's nervous system is proportionate to the tumor's location and size at the time of diagnosis. Some consideration criteria for classifying tumors have been used in this thesis. One of these factors is insufficient to make a conclusion about tumors, hence these criteria only produce useful results when they are combined.

a. Image contrast: If the segment-in this case, a tumor-appeared with white matter and the tissues around it were being pushed away from it, that would be a condition. In other words, the image's closest portion is depicted as a black area in this particular situation since the tumor is most likely benign.

b. Edema: Blood surrounding the tumor in this instance, which also manifests as very dark patches around the tumor, will increase the likelihood that the tumor is benign.

c. Contrast media: In order to color the tumor and other tissue following an MRI, the patient is given an intravenous chemical coloring medication. If the tumor reacts strongly to the contrast, it is more likely to be malignant; otherwise, it is more likely to be benign. [22].

d. Tumor contains: When tumor contains some of the following types of tissue.

i. Fat: When fat is present in a tumor and shows up as very brilliant white patches, it is likely that the tumor is malignant.
ii. Hemorrhage: when the tumor has dark patches inside of it.
iii. Fluids: When a tumor has a gray region inside of it, liquids are present, which can indicate either a benign tumor or one that is malignant.
iv. Calcifications: In extremely rare circumstances, tumors may contain some calcification, which may indicate either a benign tumor or a malignancy [22].

3.4.1 Types of Brain Tumors

According to the malignancy and healing rate grading, there are four types of cancer that can be listed as follows:

Grade i: It has the least malignancy, a higher healing rate, very sluggish cell growth, and nearly normal-looking cells under the microscope. Patients often have a good chance of surviving and, in some situations, even being cured.

Grade ii: Depending on the size of the tissues affected and the length of the disease, the cells in this grade are slow-growing and slightly abnormal under a microscope and can either be malignant or benign.

Grade iii: It has greater malignancy, faster-growing cells that appear aberrant under a microscope than grade II cells, a higher survival rate, and is still in the early stages.

Grade vi: This grade is the worst of them all, with cells that are dividing quickly, tissue that appears abnormal under a microscope, and rapidly expanding blood vessels. Patients in this grade are in a highly perilous situation, with a very low survival rate and a high rate of patient deaths [22].

3.4.2 Tumor Modalities

It is not easy to separate a brain tumor from the surrounding tissues due to the factors:

a. The disorganized brain tissue surrounding the tumor mass as a result of tumor growth, which produces a variety of gray colors.
b. Edema, who mainly manifests as white margins surrounding the tumor and may contain swelling cells around the tumor and will appear as white matter in the MRI, can sometimes cause swelling and infiltration of brain tissues.
c. The progressively developing mutation between the tumor, surrounding brain tissue, and edema results in hazy boundary detection [15].
d. Flair in MR imaging that standard appears white in imaging for delineating any tumor in the brain, as well as the blood vessels appearing as a brilliant regains also for that the information that acquired from extraction is not always as clear as desired and it is.

almost not possible to segment small area from MRI by thresholding image intensity [15].

3.4.3 Tissue Density and Image Type

The tissue that can be seen on a brain MRI has a variety of characteristics, including the following:

i. Proton Density (PD): When the image brightness is determined using the proton (hydrogen), the tissues that are rich in protons will typically have significant intensity signals, making them look bright.
ii. (T1 and T2) Magnetic Relaxation time: Magnetization generates tissue while a patient is undergoing an MRI by putting it in an unstable state, then allowing it to recover. The first condition places tissues under stress, therefore when they are allowed to unwind during the recovery period, this mode—known as the relaxation period—can be used to discriminate between diseased and normal tissues. The T1 and T2 relaxation durations that each tissue characteristic is represented by can be used to construct an MRI image. The source of contrast

that predominates is difficult to exploit, One of these two traits would serve as a fairly direct source of contrast. It is recommended to combine all three sources (PD, T1, and T2) because using just one of them will substantially weight the image. However, when an image is labeled as T1-weighted, it indicates T1 is predominate but there is also some PD and T2 contamination [20].

iii. Images with Fluid Movement: Even without contrast chemicals, MRI may detect fluids in motion, such as blood. Since fluid flow is frequently observable in all types of imaging, it increasingly serves as the primary source of image contrast, particularly in vascular examinations.

When producing MRI images, it is occasionally quite easy to see both perfusion and diffusion [20].

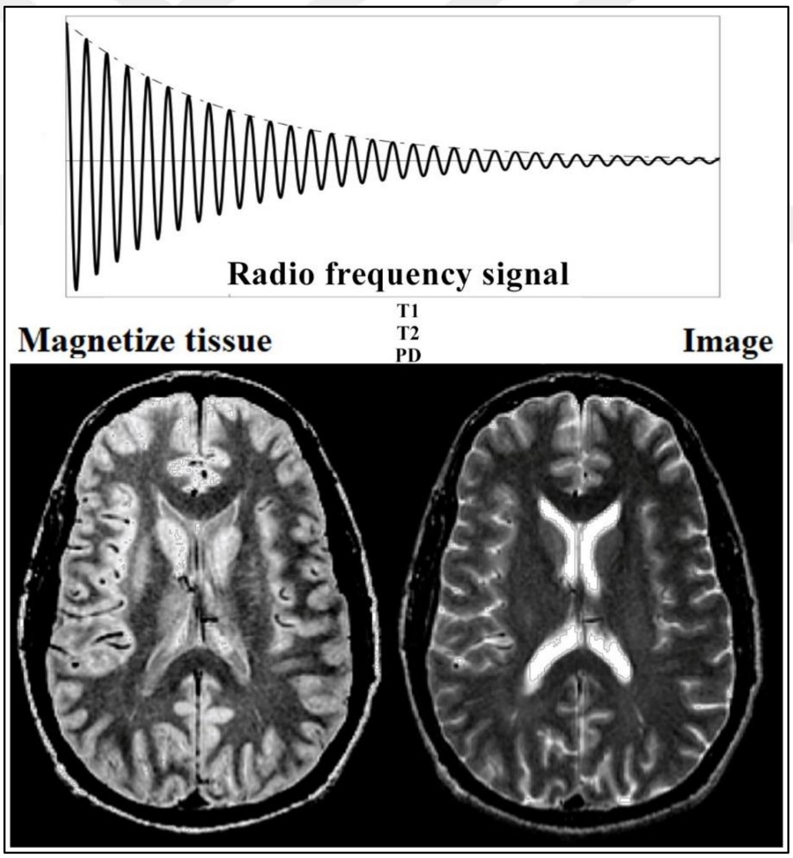

Figure 3.16: Magnetic reasoning image of the brain [20].

3.4.4 MRI Modalities

In magnetic resonance imaging, a "sequence" refers to a precise order of gradients and radiofrequency pulses that produces a particular form of image. Common MRI sequences include T1- and T2-weighted scans, Fluid Attenuated Inversion Recovery (FLAIR) scans, and proton density scans (PD). Before proceeding on with the sequences, it will first be necessary to establish a considerable number of radiology-specific jargon words:

The repetition time is the interval between two consecutive pulse sequences delivered to the same slice of tissue. The duration being discussed here is measured in milliseconds (TR). Time between the delivery of a radio wave pulse to a tissue and the subsequent reception of an echo signal (TE). The Repetition Time and Time to Echo fields have different values, and by combining these values, MRI sequences are generated. As a result, the following propositions are available to us:

a. Short TR and short TE are also used to create T1 weighted images. This modality quantifies the speed at which the tissue magnetizes. As a result, the T1 characteristics of the tissue, which outline its primary clinical distinctions, determine the contrast and brightness of the image:
i. High fat signal.
ii. MRI contrast agents, for example, exhibit strong signals for paramagnetic materials. Gadolinium is a common contrast agent for T1-weighted imaging. On T1-weighted images, it is a non-toxic substance that seems to be highly brilliant. For this reason, studying vascular architecture and blood-brain barrier breakdown with T1-weighted imaging augmented with gadolinium is highly helpful.
iii. Lower signal for the content was mostly water-based, including edema, tumors, and bleeding.
b. T2 weighted images: When creating T2-weighted images, the TR and TE are lengthened. The contrast and brightness of the image are determined by the T2 properties of the scanned tissue. As a result, when contrasted to T1 weighted images, this modality, which basically evaluates how rapidly the tissue loses its magnetization, has the opposite clinical distinctions:
i. A sequence with a high signal for increased water content can see edema, tumours, infarctions, infections, and inflammation.
ii. Reduced fat-related signaling.
iii. In the presence of paramagnetic substances, the signal will be weaker (MRI contrast agents).

In general, the appearance of the CSF fluid makes it simple to distinguish between T1 and T2-weighted images. Cerebrospinal fluid appears dark on T1-weighted images but bright on T2-weighted images.

c. Also utilized extensively is the fourth technique, known as fluid attenuated inversion recovery (FLAIR). T1-weighted sequences have longer TR and TE than T2-weighted sequences. The T1 value of a material indicates its ability to selectively attenuate or "null" signals emanating from a certain substance, in this case the fluid. This sequence is very beneficial for neuroimaging since cerebrospinal fluid is nearly always dark on FLAIR images. Clinicians use it to examine lesions such as those listed below:

i. Developing infarcts in lacunae.
ii. Plaques are an indication of multiple sclerosis.
iii. A stroke resulting from hemorrhage.
iv. Meningitis.

d. Proton density (PD): Proton density (PD) weighted images are usually utilized for imaging the brain and joints. To achieve a high-quality image with the PD weighting method, the T1 and T2 phases must be turned off. This mode provides a visual representation of the density of the proton field by utilizing the number of protons contained inside a certain volume. Consequently, tissues with a high proton density emit a strong signal, whereas tissues with a low proton density emit a weak signal.

i. The signal intensity in fat is strong, but not as high as in the T1 sequence.
ii. The intensity of the fluid is somewhere in the midway, between that seen in the T2 and T1 sequences.

3.4.5 Tumour Features

The advantage of extracting features from an MRI is the ability to spot patterns that can be used in classification techniques to differentiate between different forms of brain tumors, such as metastasis, as well as tumours of different malignancy grades. Software-based digital image analysis is more accurate and efficient than untrained human analysis. Those observers can draw more accurate conclusions to make a diagnosis of a brain tumor [14].

In different stages of treatment, MRI is used to determine whether a brain tumor is cancerous and to make a final diagnosis regarding the patient. Images can occasionally be spatially diverse. Additionally, there are overlaps with normal tissues in some photos, mainly in the invading area. Glioma tumors exhibit several mixed characteristics, such as simultaneously displaying both high- and low-grade characteristics. The surgical biopsy is necessary for the classification of brain tumors; however this classification frequently relies on the removal of tissue from the biopsy, which can be quite dangerous [15].

It aims to build an automated tool that may aid in the examination of images of brain neoplasms by assessing the glioma grade and differentiating between various types of tissue, such as primary neoplasms (gliomas) and secondary neoplasms. This will be achieved by measuring the grade of the glioma (metastases). When it comes to making a clinical choice regarding how to initiate treatment, both of these factors are crucial. In the majority of instances, alternative approaches yield more meaningful information than traditional MRI [15].

It is vital to demonstrate the accuracy of automated tools in order to WE avoid invasive procedures such as biopsies, especially when the risks outweigh the benefits, (ii) forecast diagnoses, and (iii) strengthen the distinction's dependability. This is especially true when the tumor is diverse, making it challenging to get a representative sample with a confined needle biopsy (histological examination often takes a long period of time). In this work, spectroscopic and perfusion magnetic resonance imaging were applied to examine the tumor and the surrounding tissue in four unique locations. Numerous studies have using MRI spectroscopy to classify brain tumors and distinguish between malignant and benign forms of the disease [16].

On the other hand, other studies combined the Apparent Diffusion Coefficient (ADC) with Cerebral Blood Volume (CBV), which is used to distinguish primary neoplasms from abscesses and lymphomas. The Apparent Diffusion Coefficient (ADC) is a classification method that depends on measuring diffusion in peritumoral edema to tell the difference between malignant and benign [17-15].

a. Feature Extraction: After processing, a total of 218 measurements of the intensities and textures of the SROIs are obtained. This method employs several features, including the Laplacian of Gaussian (LoG), the Gray Level Co-Occurrence Matrix (GLCM), the Rotation

Invariant Local Binary Patterns (RILBP), the Directional Gabor Texture Features (DGTF), the Intensity Based Features (IBF), and the Rotation Invariant Circular Gabor Features (RILCF) (RICGF). In the following paragraphs, we will provide a more in-depth description of the extracted characteristics:

i. The development of filters based on the Laplacian of the Gaussian distribution is the subject of current study. The Gaussian widths under consideration are 0.25, 0.50, 1 and 2. The original image and all of these values become confused with one another. The output of the SROI region of the LoG filter is used to extract sixteen features. This includes the mean, the standard deviation, the skewness, and the kurtosis.
ii. The Gray-Level Co-Occurrence Matrix, sometimes known as the GLCM, contains sixteen more characteristics. These qualities are determined by the calculation of four textural properties "Contrast," "Homogeneity," "Correlation," and "Energy" for four distinct GLCM offsets. Various terms, including contrast, homogeneity, correlation, and energy, are widely employed to describe these features. [43]. Assuming that $P_{\underset{0}{\rightarrow}}(i, j)$ is the GLCM of an image WE(x, y) within the region I_B.

b. Feature Selection: It is termed extraction to pull usable information out of a digital image, like an MRI, but after that step, features are analyzed to take the most useful feature. This step, known as feature selection, is used when the image data that has been inputs to the algorithm to be processed is too large with less useful information (large amount of data, but less information). In this case, the input data must be reduced to less amount of data that being more useful, sometimes known as feature vector transforming data that being inputs into a set of features called feature extraction when the feature that been extracted from an image carefully chosen. The term for this is feature selection [18].

This method of choosing a small subset of features from a large number of irrelevant features enhances learning performance somewhat.

i. Simplifying the dimensional issues.
ii. Increasing the capacity for generalization.
iii. Learning will happen much more quickly.
iv. The model of interpretability will be enhanced.

In addition to everything said above, the feature selection will also assist users in providing a better understanding of their data by indicating which features are more crucial for information extraction and which images are more trustworthy than others [19].

3.4.6 Brain Tumour Estimation

This crucial segmentation step will compute the tumor's area relative to the entire image after it has been removed from the original MRI (brain area). One must follow various processes in order to compute this area:

i. Reading the grayscale or input MRI image.
ii. Converting the input image to a grayscale image by formatting the weighted average of the three values (RGB), keeping the brightness but removing the hue and saturation information. The image will then be restored to one variable and put back into gray scale mode.
iii. Figuring out how many pixels there are in each row and column.
iv. Giving the parameters their initial values [12-21].

Some consideration criteria for classifying tumors have been used in this thesis. One of these factors is insufficient to make a conclusion about tumors, hence these criteria only produce useful results when they are combined.

a. Image contrast: If the segment-in this case, a tumor-appeared with white matter and the tissues around it were being pushed away from it, that would be a condition. In other words, the image's closest portion is depicted as a black area in this particular situation since the tumor is most likely benign.
b. Edema: Blood surrounding the tumor in this instance, which also manifests as very dark patches around the tumor, will increase the likelihood that the tumor is benign.
c. Contrast media: In order to color the tumor and other tissue following an MRI, the patient is given an intravenous chemical coloring medication. If the tumor reacts strongly to the contrast, it is more likely to be malignant; otherwise, it is more likely to be benign. [22].
d. Tumor contains: When tumor contains some of the following types of tissue
i. Fat: When fat is present in a tumor and shows up as very brilliant white patches, it is likely that the tumor is malignant.
ii. Hemorrhage: when the tumor has dark patches inside of it.

iii. Fluids: When a tumor has a gray region inside of it, liquids are present, which can indicate either a benign tumor or one that is malignant.
iv. Calcifications: In extremely rare circumstances, tumors may contain some calcification, which may indicate either a benign tumor or a malignancy [22].

3.4.7 Brain Tumour Datasets

Brain Tumor Segmentation (BraTS) 2022 is searching for the most up-to-date information regarding the RSNA-ASNR-MICCAI BraTS 2021 challenge in order to utilize the Synapse platform's automated ongoing benchmark for algorithmic advancements. This will allow the team to maximize the potential of the benchmark. The objective of the BraTS 2022 study is to identify the best efficient segmentation algorithms for brain diffuse glioma patients and their subregions. This will be achieved by analyzing a dataset of underserved SSA patient populations with brain adult-type diffuse glioma that was separately obtained from multiple institutions. This research is being conducted to determine which techniques are most effective for segmenting the subregions of the brain affected by diffuse glioma. Patients diagnosed with brain cancer are scanned with multiparametric magnetic resonance imaging (mpMRI) for the goal of supplying data for this competition. Through Synapse, users always have access to all training and validation data utilized for the RSNA-ASNRMICCAI BraTS 2022 competition. Before the submission time concludes in July 2022, researchers will utilize these data to create, containerize, and analyze algorithms using data from 2021's top-secret testing, data from the AfricaBraTS population, and data from pediatric patients. The most effective strategies for each of these categories will be described in full in a subsequent report. The ground truth reference annotations for each patient included in the training, validation, and testing datasets are created by neuroradiologists with extensive experience. Before these annotations can be used to conduct a statistical analysis of the performance of the participating algorithms, neuroradiologists must review and approve them. People have the option of committing all of their energies to a single cause or dispersing them over a variety of initiatives.

4. PROPOSED METHOD

The proliferation and development of abnormal brain cells can lead to the formation of a brain tumor. The vast majority of tumors can be classified as either malignant or benign, depending on the characteristics that distinguish them. Primary brain tumors are those that originate in the brain, whereas secondary brain tumors are those that have spread to the brain from another region of the body. Both of these subtypes of brain tumors can be distinguished from one another (brain metastatic tumors). Any kind of brain tumor has the potential to cause damage to a variety of different parts of the brain in addition to a wide range of symptoms. This is true despite the many types of tumors. Because of advancements in imaging technology, brain tumors can now be identified and located in the patient's head. Imaging modalities are utilized in a variety of diagnostic approaches, such as computed tomography scans and magnetic resonance imaging exams (MRI). The planning of the resection could benefit from the utilization of various MRI sequences; this would depend on the location of the tumor in respect to the normal neural pathways of the brain. In addition to this, intraoperative MRI is utilized in order to simplify the removal of tissue samples as well as cancerous growths. The chemical profile of a tumor can be examined by using a technique known as magnetic resonance spectroscopy (MRS). After that, one can use this profile to determine the location of lesions discovered by MRI. After initial therapy, a brain cancer that has spread to other parts of the body can be found with the help of a PET scan.

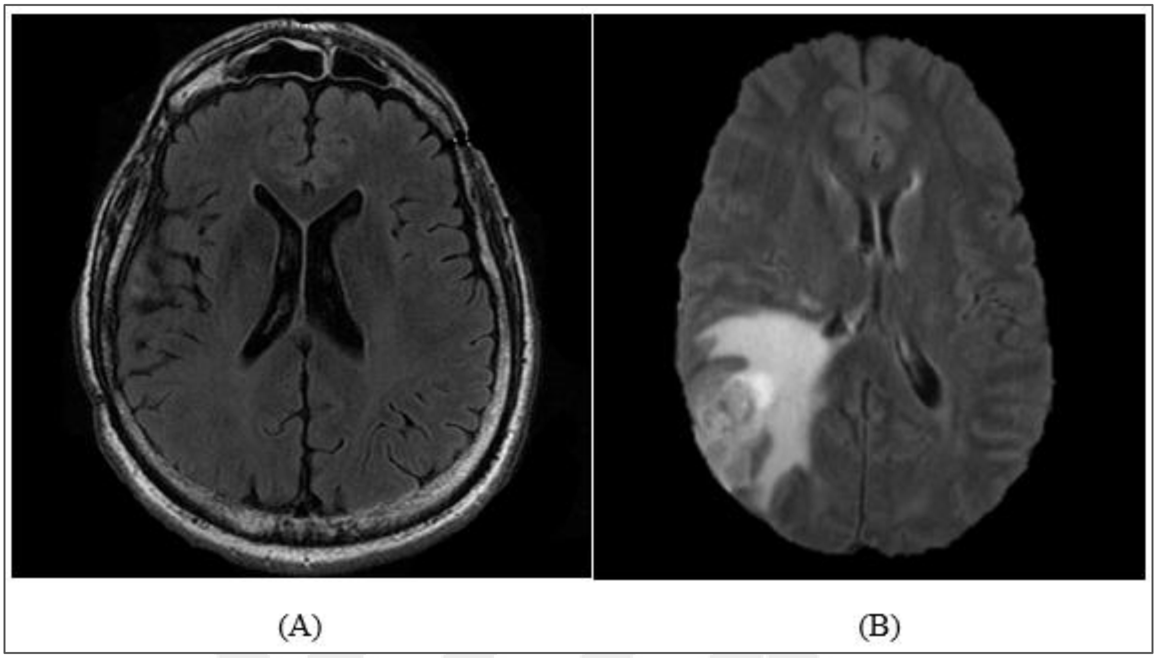

Figure 4.1: A: normal brain MRI image. B: brain with tumour MRI image

Finding the precise location of the tumor in the patient's brain was the primary purpose of the watershed and threshold procedure. When it was first conceived, this was the primary goal that the approach was intended to accomplish. This cutting-edge technology may, in just three easy steps, determine the precise location of a brain tumor and divide it into more manageable parts. Because of this, the excision of the tumor can be carried out in a more effective manner. After the picture quality has been improved, morphological operators will be utilized to zero in on the specific site of the tumor in order to remove the cancerous growth surgically. This will be done in preparation for the next step of the process. An operation will be performed to enhance the image and reduce the possibility of overlap between previously divided sections before beginning the segmentation method. This will be done before beginning the procedure to segment the image.

STEP 1: we will read the image of the brain affected by the tumor in MATLAB, and we will take its dimensions, length and width,

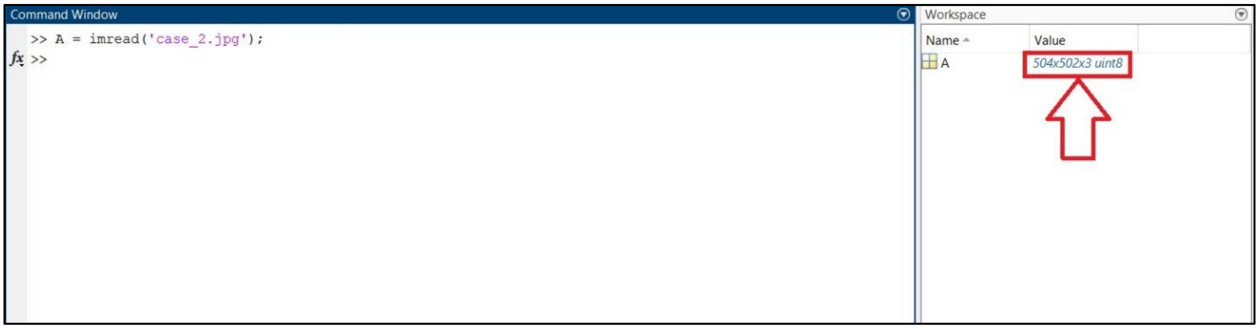

Figure 4.2: determine the size of the image (length and width) in MATLAB.

STEP 2: The second stage is represented in Maya by creating a whole floor with the same dimensions as the MATLAB image, then adding the brain image as a terrain and adjusting its height.

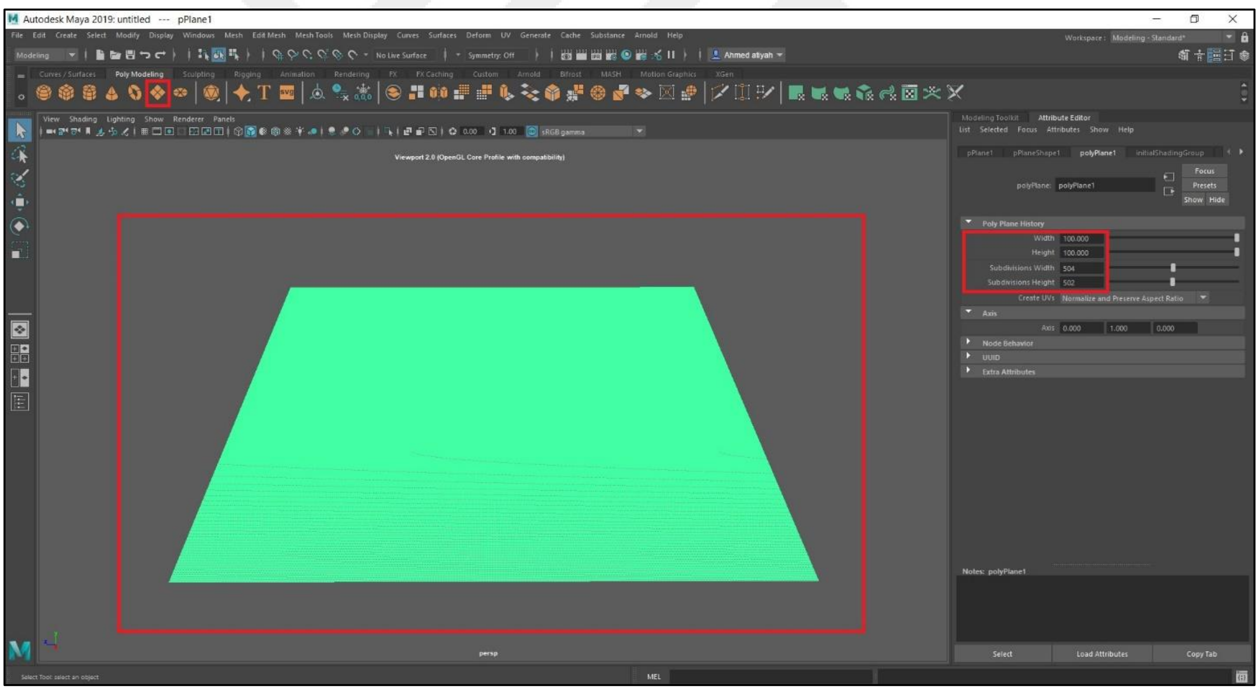

Figure 4.3: Creating a ground plane same dimensions from MATLAB.

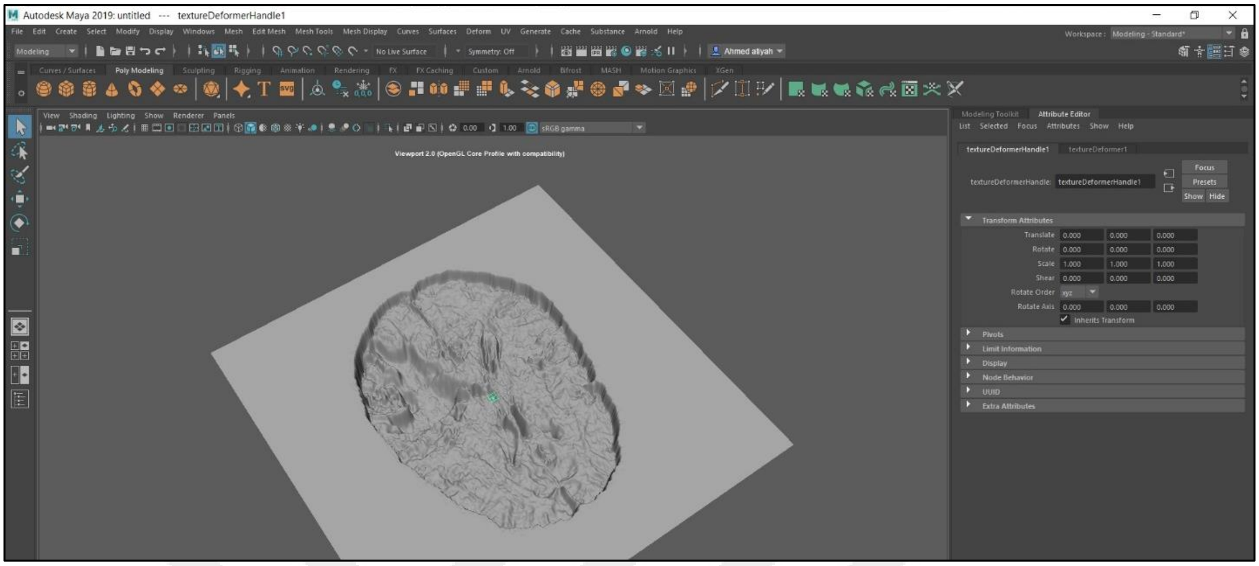

Figure 4.4: Applying height map of the brain image.

STEP 3: we create a second layer with the same dimensions and number of pixels and to control it according to the dimensions of the brain, and then we give lighting to all aspects of the work and we tweak the design from the other side to get the shape of the tumor in a stereoscopic and three-dimensional way, and the rest of the brain details remain on the other side, more precisely the second layer represents the water in The topography of the brain and the area of the tumor (the depression or the existing valley) in which the water will collect and we will get the exact tumor.

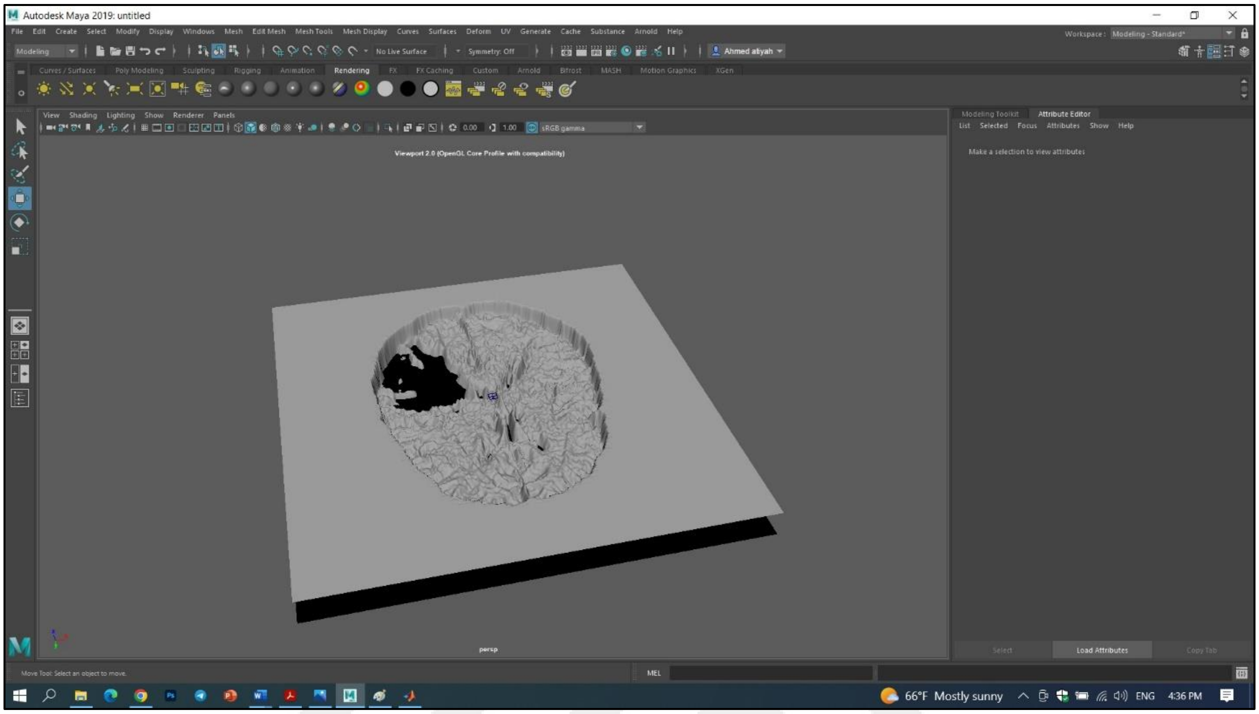

Figure 4.5: Creating a second layer to detect tumour.

Figure 4.6: Displacement of the tumour on the other side of the plane.

4.1 DATASET SAMPLING (MATLAB)

The training, validation, and testing data for this year's BraTS challenge are multi-institutional routine clinically-acquired multimodal MRI scans of glioblastoma (GBM/HGG) and lower grade glioma (LGG), all with a pathologically verified diagnosis and an accessible OS. Compared to BraTS'18, the datasets that will be used in this year's competition have been augmented with a larger number of routinely obtained 3T multimodal MRI scans accompanied by ground truth labels supplied by experienced board-certified neuroradiologists.

Brain Tumor Segmentation (BraTS) has always given a lot of attention to the evaluation of cutting-edge techniques for the segmentation of brain tumors in multimodal MRI data. This has been the case since the beginning. BraTS 2020 makes use of pre-operative MRI images obtained from a variety of institutions and focuses in particular on segmenting (Task 1) brain tumors, more especially gliomas, which are inherently varied in their characteristics (in appearance, shape, and pathology). In addition, BraTS'20 places an emphasis on the prediction of patient overall survival (Task 2) and the differentiation of pseudoprogression and true tumor recurrence (Task 3) through integrative analyses of radiomic features and machine learning algorithms. This is done with the intention of determining the clinical relevance of this segmentation task. The final objective of the BraTS'20 project is to analyze algorithmic variability in tumor segmentation (Task 4).

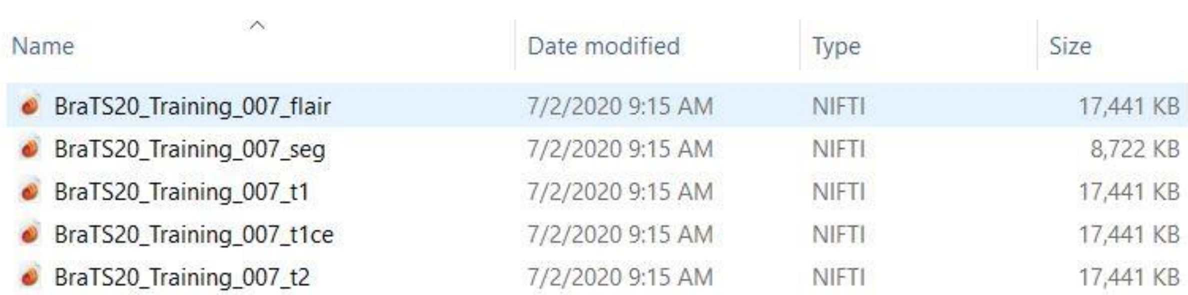

Figure 4.7: Dataset Model for each case

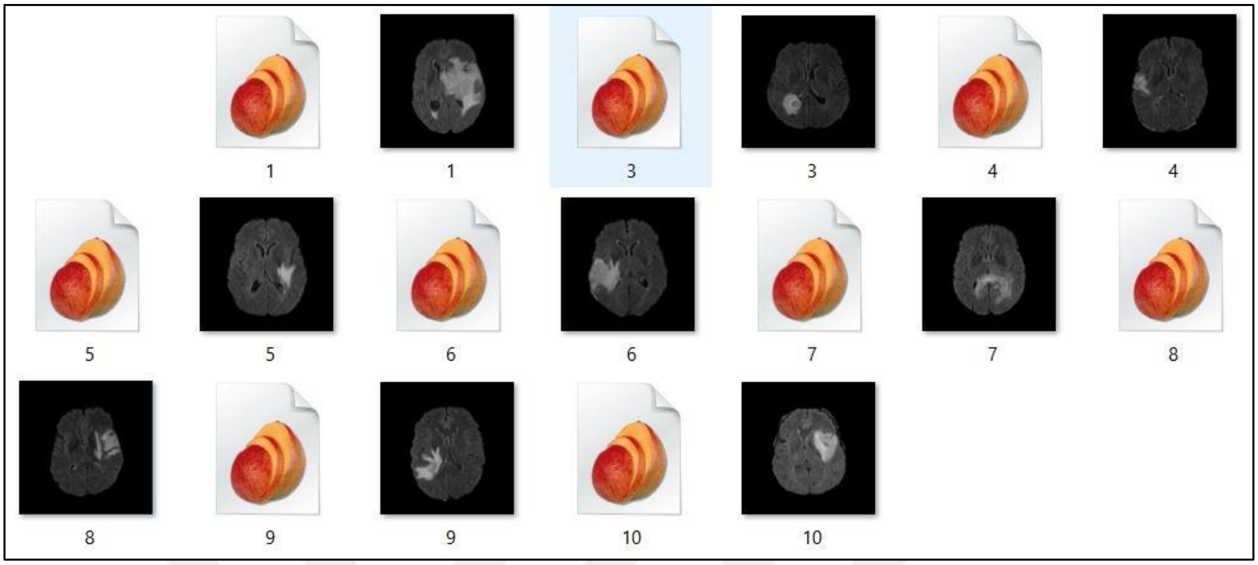

Figure 4.8: Dataset after normalization.

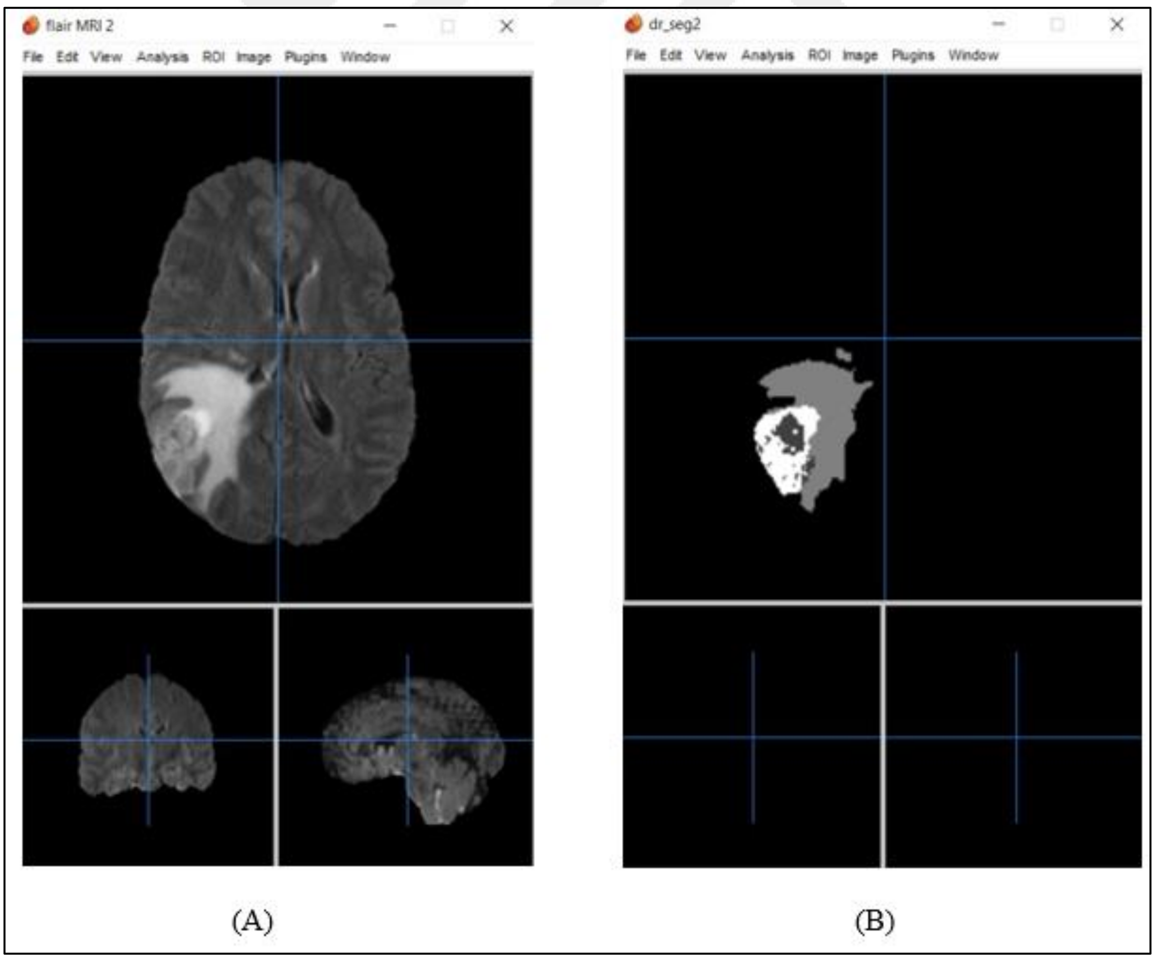

Figure 4.9: Flair MRI image Brain tumour B: doctor segmentation tumor.

4.1.1 Imaging Data Description

All BraTS multimodal scans were collected utilizing distinct clinical methods and scanners at various (19) distinct institutions. These scans are now accessible as NIfTI files (.nii.gz) that characterize native (T1) and post-contrast T1-weighted (T1Gd), T2-weighted (T2), and T2-FLAIR (T2-fluid-attenuated inversion recovery) volumes.

After being manually segmented by one to four raters using the same annotation technique across all imaging datasets, the annotations were brought to the attention of professional neuro-radiologists who validated them. In accordance with the BraTS 2012-2021 TMI article and the most recent BraTS summary paper, annotations include the GD-enhancing tumor (ET; label 4), the peritumoral edema (ED; label 2), and the necrotic and non-enhancing tumor core (NCR/NET; label 1). (please refer to section 4.3 as well) The provided data are made available for public use after being preprocessed as follows: they are co-registered to the same anatomical template, interpolated to the same resolution (1 mm3), and stripped of skull information.

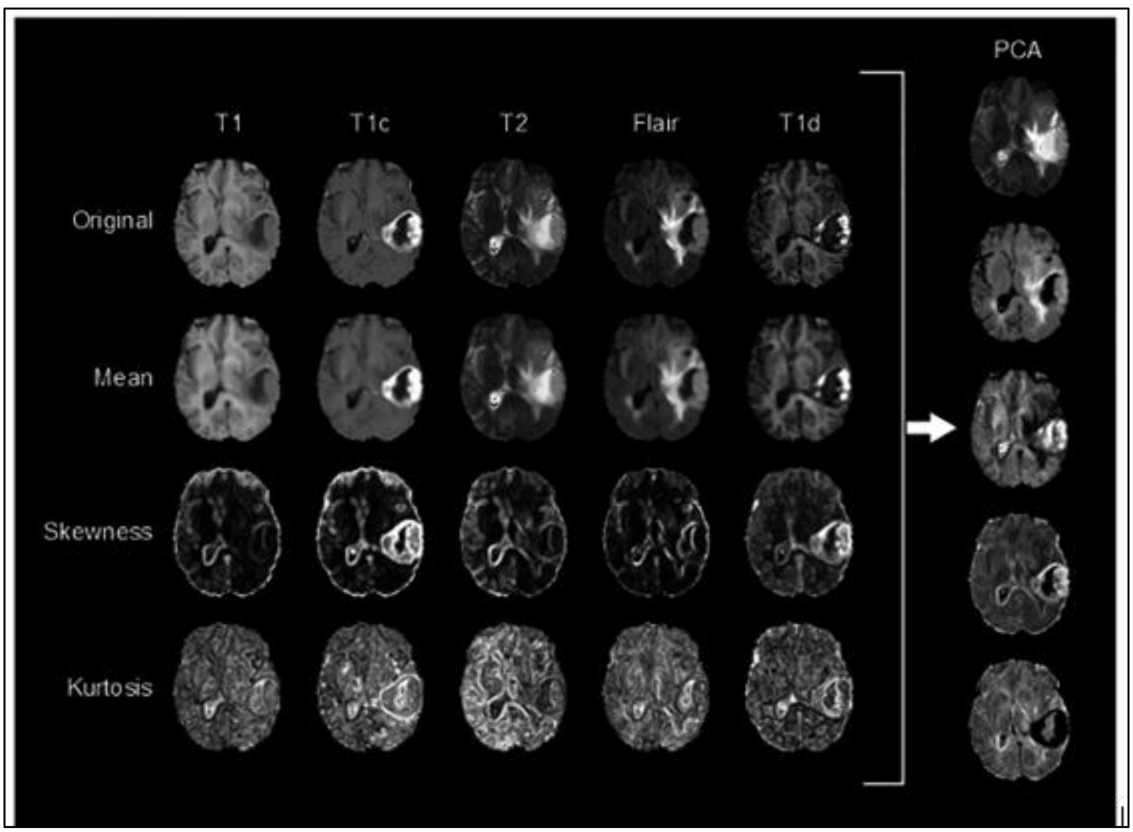

Figure 4.10: Modalities of the brain tumour dataset BRATS2019.

4.1.2 Comparison with Previous BRATS Datasets

It is abundantly clear that the BraTS data supplied after BraTS 2017 and the BraTS data provided in past tournaments are significantly distinct from one another (we.e., 2016 and backwards). Images and annotations from BraTS'12-'13, which were manually annotated by clinical specialists in the past, are the only data that have been utilized earlier and are being used again (during BraTS'17-'19). These are the only information utilized. Because the ground truth labels for the scans described in BraTS'14-'16 (from TCIA) were annotated by combining the segmentation results of algorithms that ranked highly in BraTS'12 and BraTS'13, these datasets were deemed meaningless and discarded. Consequently, the labeling were erroneous. The original TCIA glioma collections (TCGA-GBM with 262 cases and TCGA-LGG with 199 cases) have been radiologically inspected and classified as pre- or post-operative by a team of trained neuroradiologists in preparation for BraTS'17. Then, all of the pre-operative TCIA scans (135 GBM and 108 LGG) were incorporated in this year's BraTS datasets, and specialists annotated them for the multiple glioma sub-regions present.

The Cancer Imaging Archive (TCGA) now contains the naming convention and filename mapping between the BraTS'19, BraTS'18, and BraTS'17 datasets and the TCGA-GBM and TCGA-LGG collections. Previously, this was unavailable (TCIA).

4.2 PREPROCESSING (MATLAB)

Multiple noise sources can degrade MR images. Both image compression and transmission have the capability of introducing noise to the final image. In this study, both nonlocal means and local smoothing approaches were combined to minimize background noise. Due to the fact that vital image structures and details frequently appear to be noise, it is possible that they will be eliminated throughout the editing process. The most significant phase in the analysis of images and forecasts is the creation of records. This is because erroneous input, such as undesirable statistics, might contribute to a classifier's poor performance. Due to the heterogeneous character of the collection, in which MR images of differing widths and heights coexist, it is necessary, as a first step, to develop a visual representation of the distribution of these dimensions. In order to accomplish this, a visual representation of the distribution must be created. There is an illustration of line plots, which compare the length and height of a data collection, within the parentheses. Because the width-to-height ratio is inconsistent, as depicted in Figure 4.11, and the great majority of photos have a height-to-width ratio that is less than 1, scaling the images is a necessary step prior to identifying the tumor's elegance.

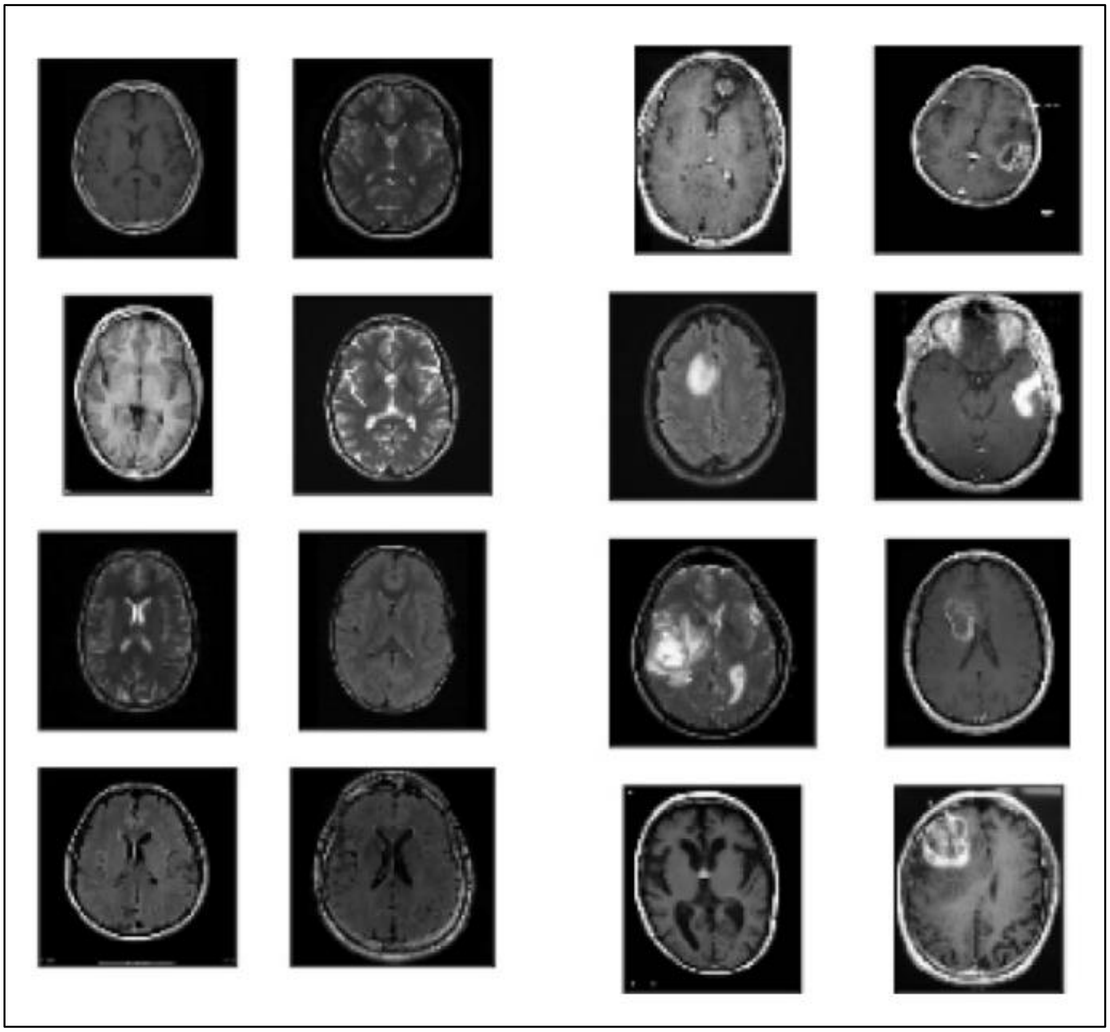

Figure 4.11: Resizing the image.

4.2.1 Cropping (MATLAB)

It's probable that the performance of the proposed segmentation is due to the presence of a number of unwanted regions and empty spaces, both of which are present in virtually all images. As a result, it is vital to crop the images in order to guarantee that they only reveal the pertinent information and eliminate any extraneous clutter. Using Rosebrock's method, which involves calculating the image's extreme points and constructing its contour, the parts of the image to be cropped are determined (2020). To show how to crop photos by identifying the image's most significant areas, we shall proceed as follows: After completing Step 1, which entails loading the original images and resizing them to a size of 224 by 224 by 3, you will proceed to Step 2, which involves applying erosions and dilations to the image's small parts. After finding the perimeters of the threshold images, the fourth step is to select the image with the largest overall area. Locate the four corners of the images in Step 5. (upper left, lower right, upper and lower left). After fusing the contour and extreme points, proceed to step six, cropping the images.

4.2.2 Resizing the Image

To acquire the best possible results from a dataset, it is required to resize the images so that they all have the same height and breadth. When resizing images, care must be given to preserve as much of the original image's quality and detail as possible. This study entails enlarging the MR images in width, height, and channel (224 224 3), with the selection of these dimensions being prompted by the fact that our proposed model employs a comparable architecture to that of Regular watershed, which employs an input layer of 224 224. This study also entails enlarging the MR images in width, height, and channel (224 224 3), with the selection of these parameters influenced by the need to resize the images. It is recommended to train the AI model using a sizable dataset in order to prevent the difficulties caused by overfitting. In addition, the effectiveness of the DL model may be much enhanced if it were trained using the massive dataset. Data augmentation refers to the procedure of generating a new dataset by modifying an old one (DA). Using DA, it is also feasible to generate multiple copies of the original image in a number of other orientations. This work resulted in the development of a total of 21 digitally enhanced photos, with each image acting as the basis for a new image after undergoing minor modifications. Figure 6 displays the primary image as well as 21 enriched variants of it. The base image is displayed at the top, followed by the variants with the augmentations.

4.3 SEGMENTATION USING 3D WATERSHED

4.3.1 Creating The 3d Plane (MAYA)

The Plane is a height field that possesses each of the qualities listed below.

i. Resolution

This parameter specifies the number of samples in relation to the largest side length of the plane. By increasing the resolution, more surface detail will be visible. Reduce the resolution to increase the playback speed.

ii. Color

Sets the color that will be used for the preview plane's surface. You can map the color either to the surface texture or to the Ocean shader. Even if the mapping is applied to a different attribute, the mapping will always use the out-Color from the related node.

iii. Displacement

Here, the plane's height can be modified. The displacement mapping occurs within the Ocean shader. The mapping always uses the outAlpha value of the connected node, despite the fact that a different property may be associated. This does an ideal analysis of the texture, during which additional shading engine inputs are ignored.

iv. Height Scale

Adjusts the input displacement's magnitude. This value must be increased so that the displacement is more apparent.

Table 4.1: Image parameters (MATLAB).

index	width	height	Dpi	pnsr	type
Tc1	500	350	70	0.3	grayscale

Table 4.2: 3d plane parameters (MAYA).

index	width	height	rows	columns
Plane1	1000	1000	500	350

4.3.2 Applying the Heightmap (MAYA)

A cool technique for producing a landscape in Maya is to utilize the "texture deformer" tool in conjunction with a height map. In a bitmap image saved on a disc, the height of a pixel is represented by its luminance in the form of a height map. This height is measured in relation to a plane of level ground. Moreover, a height map can be found in numerous locations. In order to build a height map, a third-party application, such as View or World Machine, is required. When creating a height map with an image editor such as Photoshop, you have the option of hand-drawing the map or importing data from a geographic information system (GIS). So let's do that; WE have some MRI data that WE received from the BRATS dataset, and we'll use that as an example. WE intend to develop a comprehensive plan for this key region. Its exact perimeter is most likely in the vicinity of 50 kilometers. And for me to be able to work with it, Maya must modify the scale of my layout accordingly. The one-hundredth scale featured in the original film is no longer utilized. The model you are viewing is one thousand times smaller than the actual circumstance. Select the plane primitive, and then change the channel box input nodes and the polyplane node so that the object's width and height are each 5,000 centimeters. Moreover, if this is a 1:1000 scale model, the dimensions of the model would be 50 kilometers on each side. In addition, the width and height of each subdivision is set to 200 pixels. Using the height map method, both the number of sub-regions and the level of information can be modified at a later date, which is a significant advantage. By selecting the planar object from the modeling menu, access to the texture deformer is granted. Select the "Texture" option from the "Deform" drop-down menu. The texture deformer node has previously been selected, and its parameters are now displayed in the channel box; however, the texture assignment option remains disabled.

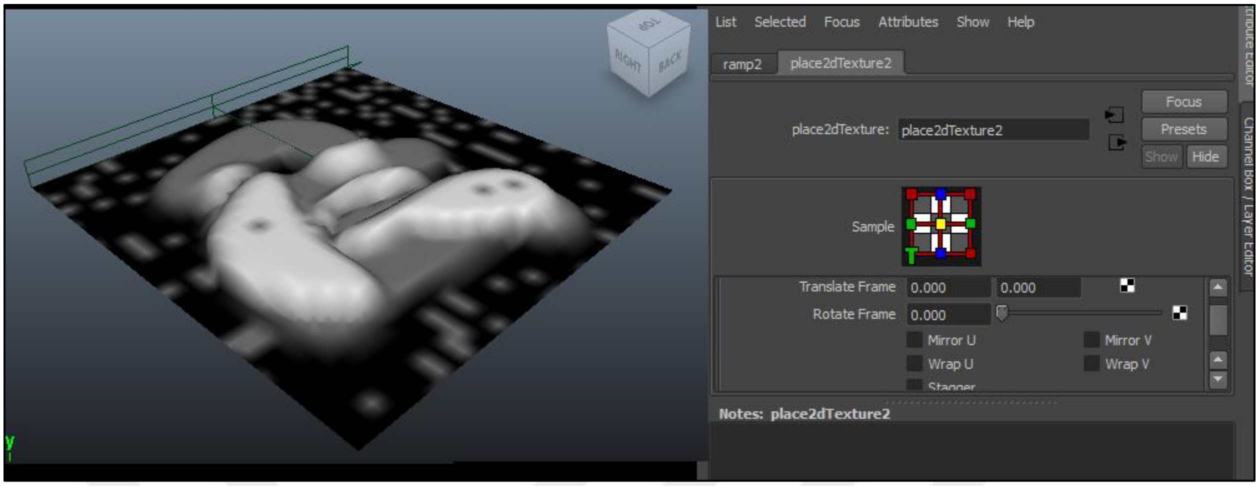

Figure 4.12: Heightmap in maya.

The attribute editor is where we would like to be at this time. To display the outcome of the attribute editor, we can therefore press the Ctrl key and the letter A. If you deselect this texture deformer window, make no selections, or make any other choices, it will close and disappear. The texture deformer disappears from the attribute editor when WE release the button that is holding down the mouse button while hovering over the object. If we deselect and then reselect an item, we shall be returned to the attribute editor's tabs. When you apply this deformer to the material, you may observe both point space and direction. As a default, the UV coordinate system will be used for the point space. The UV coordinates of the object are utilized to establish the projection of this height map onto the object. And we are pursuing a course that is not insurmountable. The word "handle" is a shortened form of "scene handle or locator," which refers to an object that can be used to change the position of the height map on the ground, as well as its orientation with regard to the ground, and other similar things. The outliner assigns it its own texture deformer handle as one of the obvious signals that it is a distinct entity. Since it is already positioned at zero, there is no reason for me to move or rotate it at this moment. WE'm going to attempt to temporarily forget about it. You must navigate back to the texture deformer's settings and then click the produce render node button situated next to the texture slot. Create a node in the note attributes of the file to record the information. To achieve the greatest results, it is advised that the filter be fully disabled. We do not wish to apply a pre-filter to the texture as we did to the matte painting. Avoid changing any of the information. Then, we will find the image by clicking the "Browse" link on the toolbar. The present project's source images folder contains a PNG file labeled height map

Wy'east 3601 by 3601 gray 16 bit. Mount Hood was always referred to as east by the native peoples of North America. The file contains 3601 squares, which represents the computer's resolution. Adding the finishing touch, the image is grayscale with a dynamic range of 16 bits. It is advised that you create height maps using either 16-bit or 32-bit images. If the image is 8 bits, there will only be 256 different elevation levels, which is not a really high quality number. We require an image with a resolution of 16 or 32 bits. This will be implemented with a single click, but the ultimate outcome will be unremarkable. The texture strength is pretty low by default, and our flat object is quite massive. As a result, we will need to increase our efforts. By selecting the plane and then the texture deformer tab within the attribute editor, it is possible to alter the amount of deformation applied to the texture. This should be increased to a total of three thousand. Due to the immense size of the aircraft, a tall tower will be required to accommodate it. There is no scale that can be utilized to compare the quality of strength. If we increase or decrease the size of our object, it is likely that we will need to adjust the amount of force we apply. This is good news; please deselect it so we can examine it. By employing the full left mouse button, we are able to roll around. From this vantage point, Mount Hood and the Columbia River are visible. We can do mouse-controlled zooming and panning by simultaneously pressing the Alt key and the Right Mouse Button on the mouse. Take this into account in your thoughts. In addition, the photograph appears to be of relatively poor quality. The lack of attention to detail is a detriment, but it is easily rectifiable. Take it out of there. We can raise the height of the subdivisions by dragging the mouse back to the channel box and then back to the polyplane node. One side of the height map file consists of 3601 pixels, as depicted. And WE would like to apply that in this scenario so that WE can collect the most information possible. WE'm sorry to disappoint you, but the polyplane will not accept such a high value. The maximum number of cells that can be accommodated is 2,000,000. It shouldn't be that difficult to solve this problem; all WE need to do is divide 3601 by 2. This yields a number that is close to 1800; WE can then enter this number into both the width and height fields and press enter. In addition, a caution notifies me that your subdivision's property values are notably high. Is this really what you wish to hear? WE would like to give you my "yes." Some time is necessary for determining this. When that occurs, we will be able to discern significantly more particular details. Remove the mouse from that object promptly and completely. And now we can orbit or tumble around to view the terrain from a variety of perspectives, and we now have a height map with a reasonable level of detail. After selecting the plane object, we return to the polyplane to determine if it is possible to minimize its size. We will be able to survive if you add 900 subdimensions in each direction. To lower the amount of memory required for this new height map, we must sacrifice certain information. In the future, it's possible that we'll need to erase the build log for this airplane. We will be able to conserve memory and disk space by lowering the quantity of data utilized for this aircraft. Utilizing a height map in conjunction with a texture deformer is the crux of the terrain creation process.

4.3.3 Shedding the Water (MAYA)

a. To render the water, you must first construct a new VRayMtl and then apply it to the utilized geometry object.

b. You should select a hue that is similar to white since the reflections in motionless, pure water are nearly as reflective as glass (200, 200, 200).

c. You can leave the Max Depth parameter of the Reflection advanced rollout at its default value of 8, or you can change it to a higher value. The maximum reflection depth determines the number of times a light is capable of being reflected. Due to the high reflectivity of water, the best values for achieving the desired effect range from 7 to 10. If water is housed in a clear glass, keep in mind that the glass itself must have the same reflection max depth parameter as the water substance. This is because this parameter is defined for the water substance.

d. Since water has a refractive index of one, white should be chosen for the Refraction Color (255, 255, 255).

e. You can leave the Max Depth parameter of the Refraction advanced rollout at its default value of 8, or increase it. Maximum refraction depth is a helpful measure for determining the maximum number of times a beam can be bent. A number in the range of seven to 10 is required to show water accurately. If the water is housed in a transparent glass, keep in mind that the glass must also have a refraction max depth parameter equal to the value you specified for the water material. This parameter must also be identical to the maximum depth of refraction parameter.

f. As a rule of thumb, you should employ a Refraction IOR of 1.33 when working with water or with substances that are predominantly composed of water. The Refraction IOR and Reflection IOR are synced automatically, and the Reflection IOR will use the Refraction IOR's value internally without your intervention.

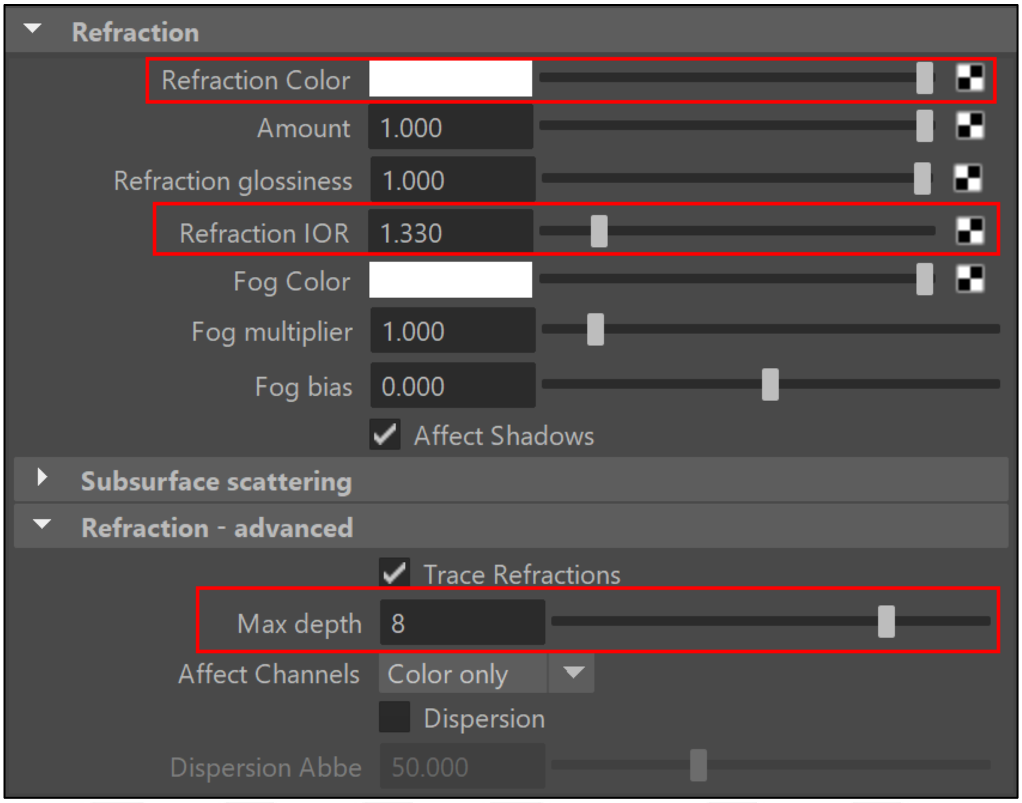

Figure 4.13: Depth and viscosity parameters of the water.

4.3.4 Calculating the Ponds Depth (MAYA)

Using a spring mesh solver and a height field, ponds are modeled as a type of two-dimensional fluid. Using the available settings and features of the pond, you may select the dimensions and color of the pond's liquid surface. When applied to the surface of a fluid, wakes have the power to produce waves, bubbles, and ripples. If you widen the pond from which the waves and ripples emanate, they will spread further. In terms of preparation, the menu items at the Pond are essentially identical to those at the Ocean. Learn more about the Pond menu by reviewing the Ocean menu's online help.

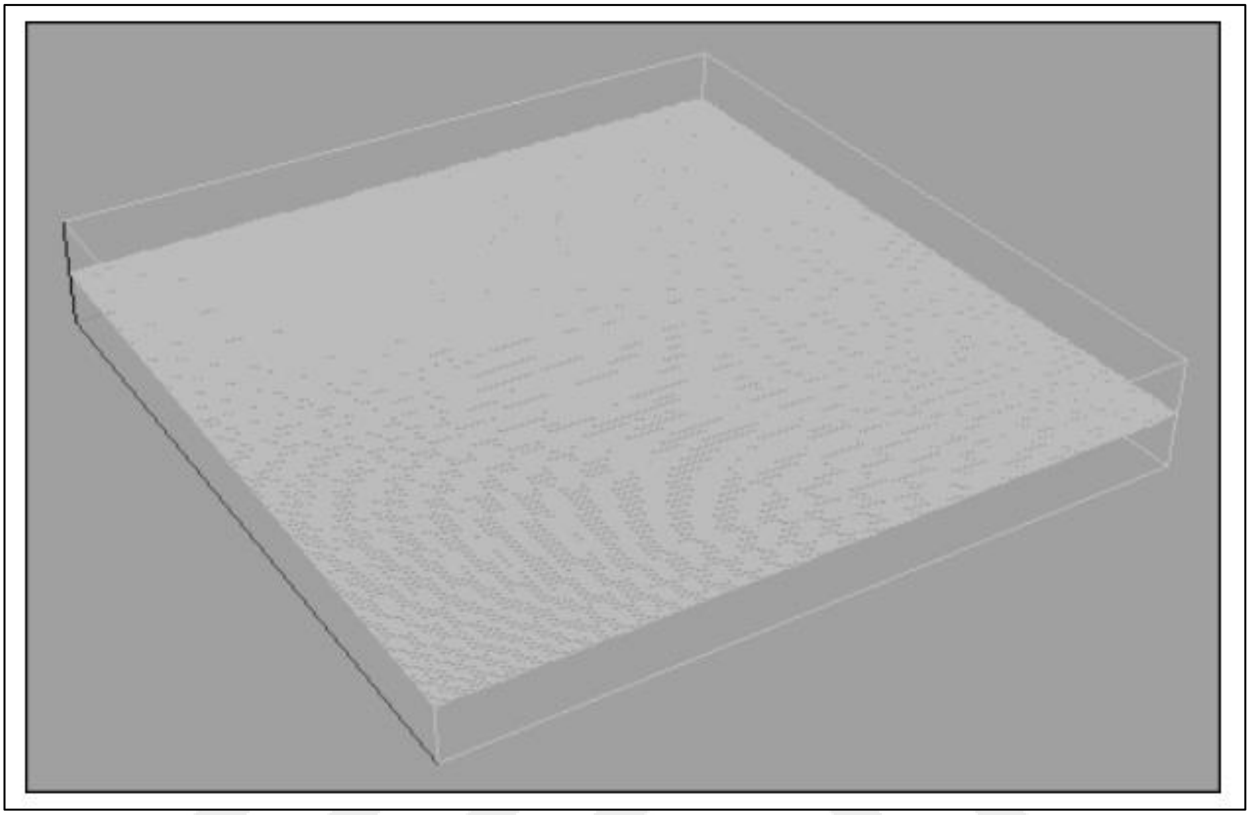

Figure 4.14: Calculating the ponds depth.

4.3.5 Extracting the Tumour with Features (MAYA)

A series of magnetic resonance imaging (MRI) scans of a brain tumor were analyzed using the proposed method. Using a number of image processing approaches, such as morphological operations, segmentation, watershed transformation, and marker-controlled watershed transformation, among others, a more comprehensive extraction of the region containing the brain tumor was accomplished.

In this experiment, the watershed algorithm is applied to a number of example images using a wide variety of feature combinations, and the resulting images are analyzed.

In Figure 4.15 the results show the isolation of the brain tumor that we obtained from the three-dimensional method, compared to the diagnosis of the specialist doctor in the second line of the figure, in addition to the third line of the figure, the whole brain imaging is shown with the tumor in flier MRI.

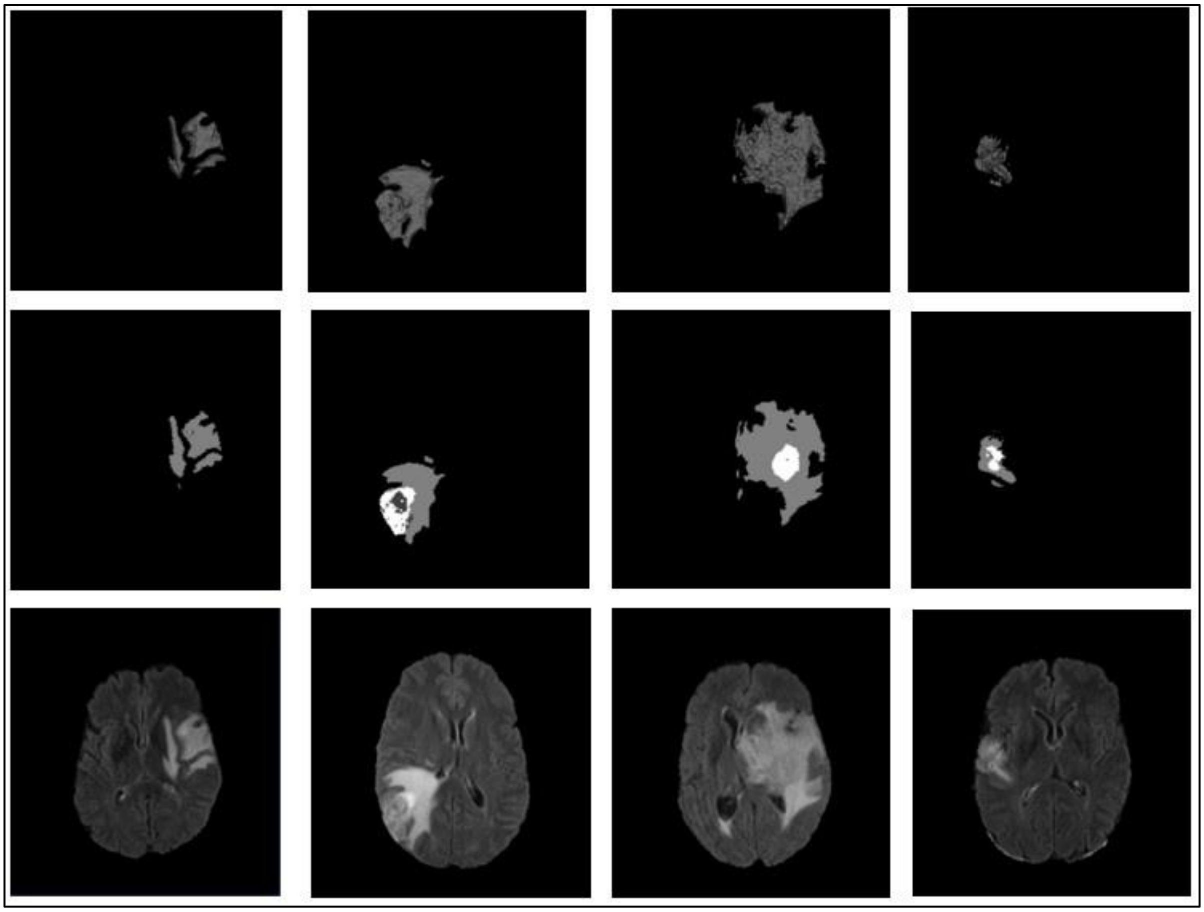

Figure 4.15: In the first line of this figure, we give the results obtained through the usage of our methodology. The classification of the tumor by the oncologist is discussed in the second line. The third and final line images from the flair MRI.

Using two different types of similarity algorithms (Dice index and Jaccard index) between the image received from the specialist doctor's diagnosis and the image created by our technology, we determined that 10 cases of brain cancer were accurately detected

Table 4.3: Dice and jaccard scores of the 10 cases.

Case No.	Thresholding	Width	Height	Subdivisions Width	Subdivisions Height	Dice index	Jaccard index
Case 1	0.1	100.000	100.000	502	504	0.9322	0.8730
Case 2	0.1	100.000	100.000	502	504	0.9524	0.9091
Case 3	0.09	100.000	100.000	504	507	0.9242	0.8590
Case 4	0.02	100.000	100.000	504	506	0.8833	0.7911
Case 5	0.05	100.000	100.000	502	502	0.9455	0.8967
Case 6	0.05	100.000	100.000	503	502	0.9296	0.8684
Case 7	0.05	100.000	100.000	505	503	0.9261	0.8624
Case 8	0.05	100.000	100.000	499	498	0.8743	0.7767
Case 9	0.1	100.000	100.000	502	505	0.9254	0.8754
Case 10	0.1	100.000	100.000	501	503	0.9354	0.8821

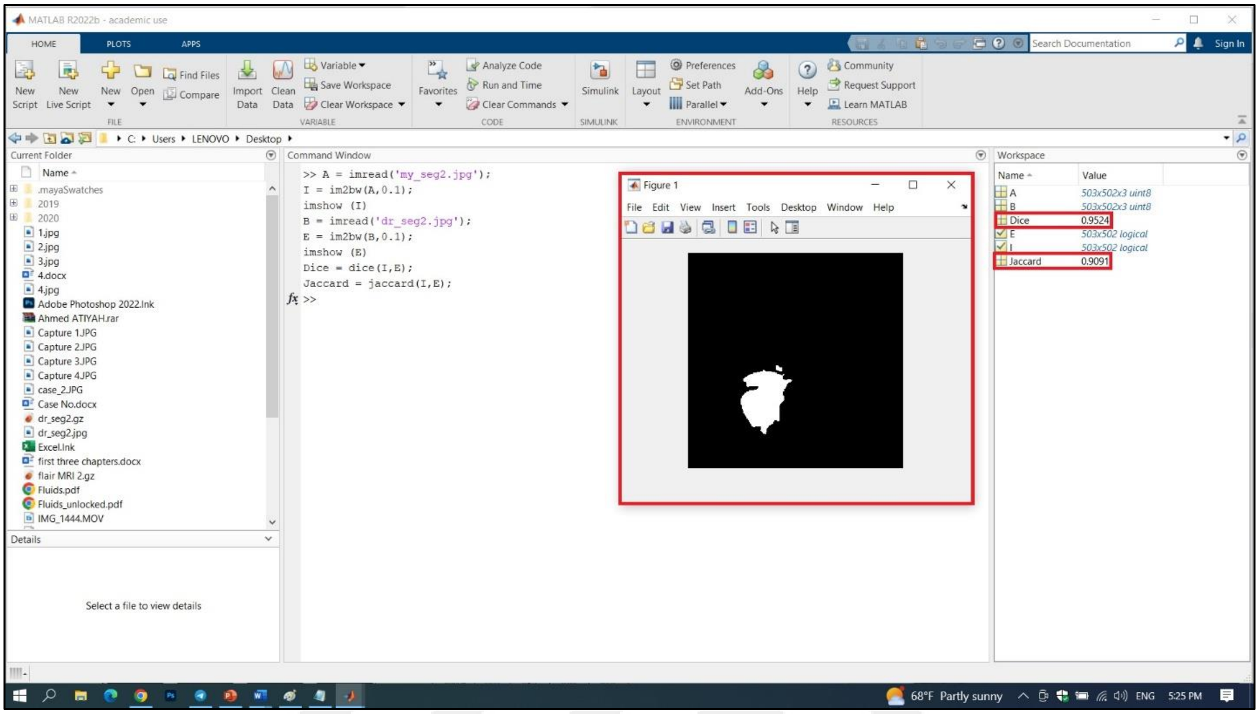

Figure 4.16: Image parameters acquired from MATLAB.

5. RESULTS DISCUSSION

In order to perform an exact comparison between our segmentation and the ground truth segmentation, we modified the traditional Dice and Jaccard coefficient metric. It has been proved that the proposed Dice coefficient is less biased and more robust than standard Segmentation techniques, as well as possessing the desired features. In contrast to the uniform ratings given by conventional Segmentation, the proposed Dice and Jaccard coefficient gives greater weight to errors that are linked with a higher degree of certainty or likelihood. We expect that this unique technique will be useful in brain tumor segmentation research as well as in the creation and evaluation of fresh techniques.

One of the things we conducted with the MRI images contained in the Brats2019 dataset was to compare the Dice and Jaccard scores of several 3D watershed and other MRI FLAIR lesion segmentation techniques. This data collection contained fifty patients. Then, we examined whether or not the precision of the 3D watershed approach is superior to that of the conventional watershed segmentation. If there was a risk of inaccuracy of 0.5 percent, the FLAIR image lesion load ratings would average 0.95, according to our estimates.

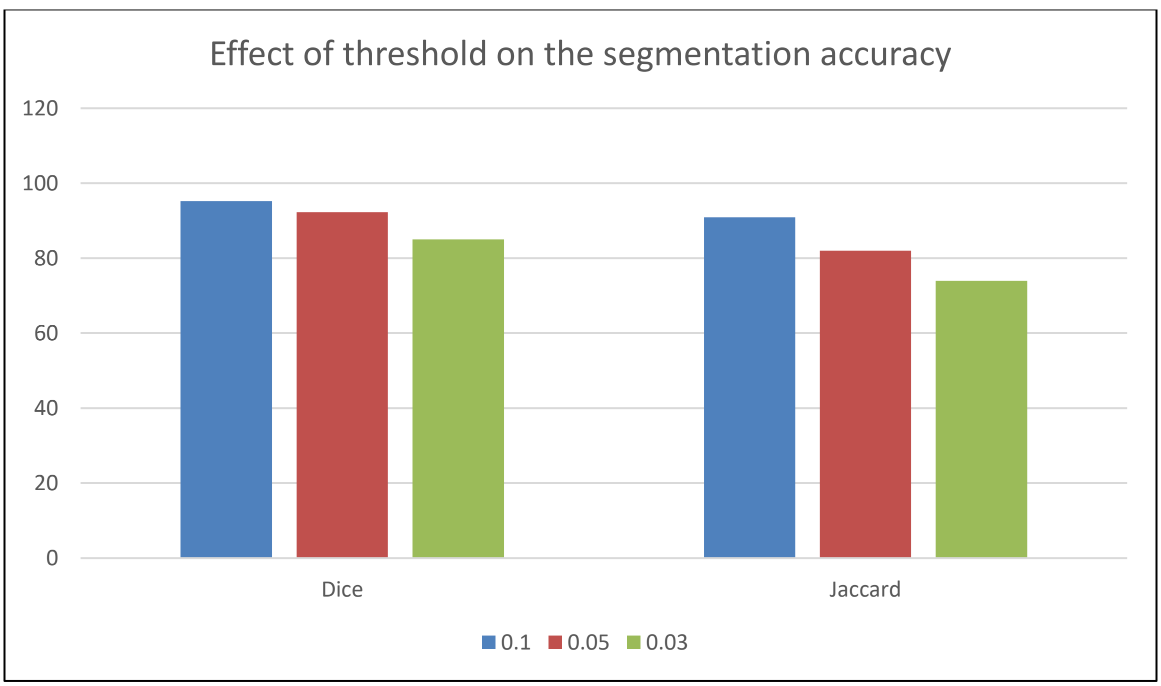

Figure 5.1: Effect of threshold on the segmentation accuracy.

The structure of the tumor, its complexity, and the segmentation threshold all contribute to varying degrees of detection variability, according to the study's findings. Depending on the characteristics of the ideal Segmentation, one may need to weigh the advantages and disadvantages of utilizing the desired model vs the commonly used alternatives Dice and Jaccard.

When a threshold of 0.1 mm was applied to either procedure, the resulting precision was exceptional. When comparing the findings of the 3D segmentation to those of other models using interscan evaluation, differences greater than 0.1 mm were found in 16 of 21 cases. If other brain tumor segmentation algorithms employ the typical segmentation threshold, they will neglect portions of the tumor. By adjusting the segmentation threshold, we were able to reconstruct previously absent brain regions and evaluate how the image quality had altered as a result of these modifications. As a result of the threshold adjustment, both the Jaccard and Dice segmentation scores attained an all-time high of 0.95.

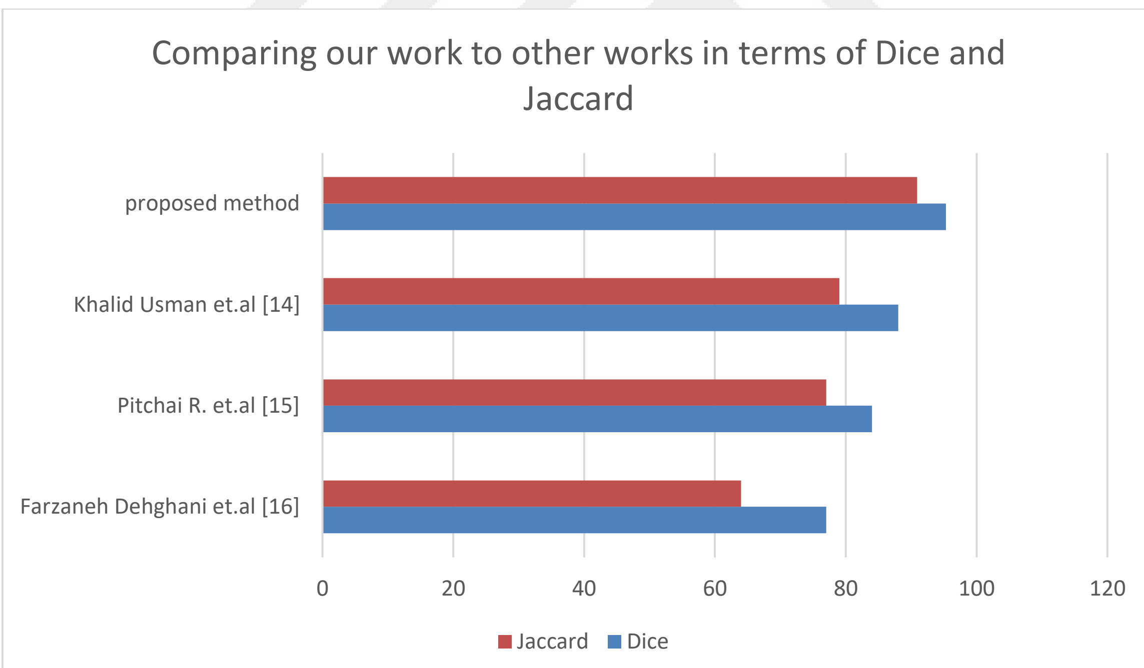

Figure 5.2: Comparing our work to other works in terms of Dice and Jaccard.

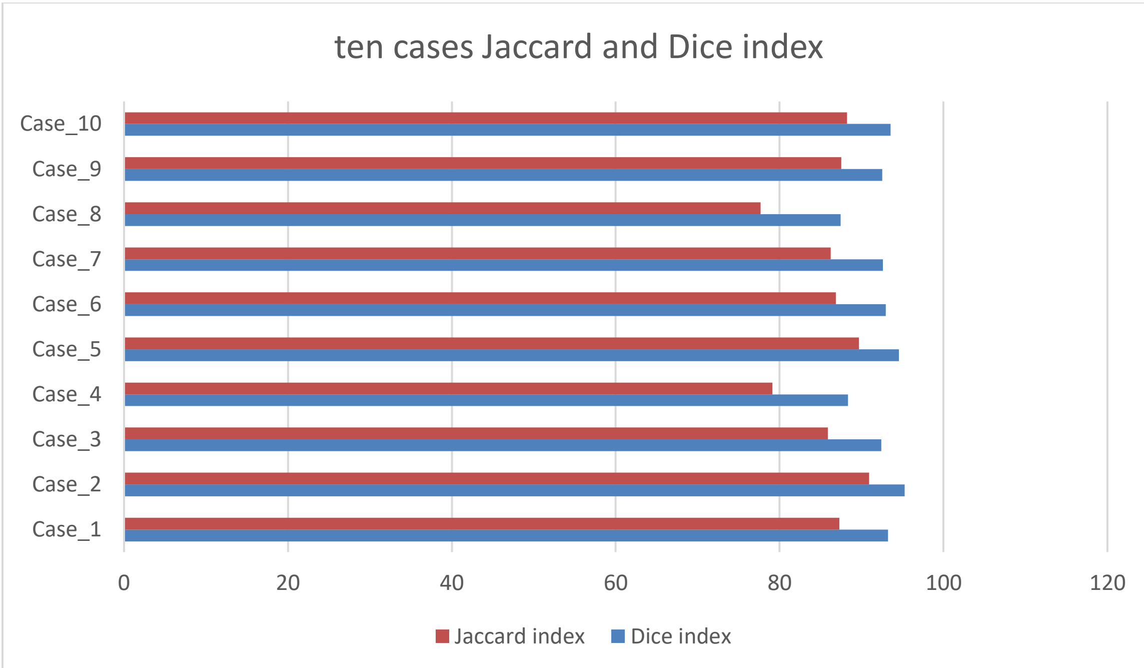

Figure 5.3: Ten cases Jaccard and Dice index.

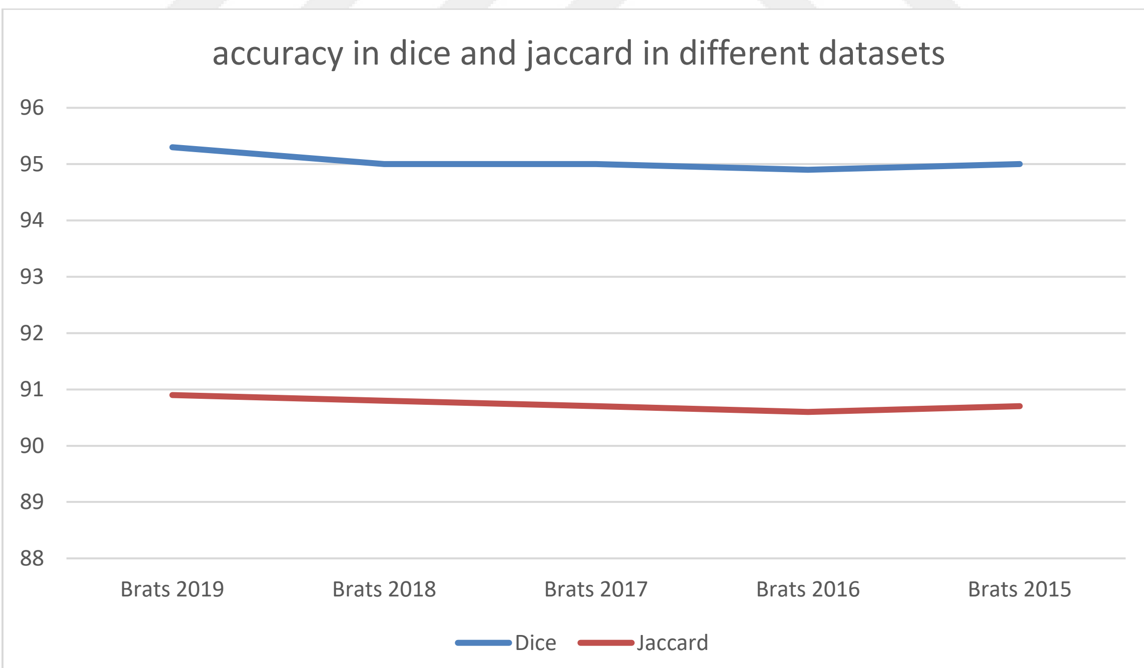

Figure 5.4: Accuracy in dice and Jaccard in different datasets.

6. CONCLUSION AND RECOMMENDATION

6.1 CONCLUSION

Digital imaging technology is becoming increasingly prevalent in the modern world, and the number of scientific disciplines that could profit from it is constantly expanding. A variety of Image altering applications have recently gained favor as efficient tools for enhancing image analysis. This tendency is anticipated to persist. By doing an analysis on the values and dimensions of each segment, a segmentation technique can be utilized to manage an image object more efficiently. Digital imaging has become increasingly important in the medical profession, with many research opting to analyze digital images in magnetic resonance imaging (MRI) format. Image analysis, pattern recognition, and even blind perception can greatly benefit from image segmentation [1]. When a cancerous tumor in the brain is diagnosed incorrectly or slowly, it will result in many problems, including aggravation of the patient's condition, spread of disease, and death. In the event that a clear image of the brain is not seen, and the location, size and type of the tumor are known, the patient will be given wrong doses, causing damage to healthy brain tissue. Due to the scarcity of doctors specialized in radiology, which delays the diagnosis time due to the momentum of doctors, the algorithm is of great importance in reducing the time and speed of diagnosis, which makes it very useful if used When working with complex medical images, segmentation is necessary for determining the region of interest for further analysis. As a result of segmenting the complete tumor profile, the initial population was very vast; however, this has been drastically decreased so that focus may be directed on a more restricted genetic group. This study's primary contribution is a reliable approach for segmenting the tumor area MRI scans to find and isolate it. First, the watershed method is used to the images, followed by a second segmentation in order to obtain the brain tumor. After including a fitness function into the algorithm, we will score the DICE and JACCARD-segmented images to assess how well they compare to one another. Segmentation is largely applied to increase image analysis and comprehension by dividing an image into portions based on one or more criteria, such as color and object. Using two different types of similarity algorithms (Dice index and Jaccard index) between the image received from the specialist doctor's diagnosis and the image created by our technology, we determined that 10 cases of brain cancer were accurately detected, When a threshold of 0.1 mm was applied to either procedure, the resulting precision was exceptional. When comparing the findings of the 3D segmentation to those of other models using interscan evaluation, differences greater than 0.1 mm were found in 16 of 21 cases. If other brain tumor segmentation algorithms employ the typical segmentation threshold, they will neglect portions of the tumor. By adjusting the segmentation threshold, we were able to reconstruct previously absent brain regions and evaluate how the image quality had altered as a result of these modifications. As a result of the threshold adjustment, both the Jaccard and Dice segmentation scores attained an all-time high of 0.95.

6.2 FUTURE WORKS

Utilizing a range of neural network topologies, researchers are urged to improve present tumor detection techniques. It would be intriguing to utilize less labeled images and watch how other neural network types (including ANN, CNN, PNN, DNN, and basic neural networks) behave and provide results. This inquiry would be evaluated based on a variety of criteria, including precision, timeliness, specificity, and efficacy, among others. To appropriately prepare for therapy, it is necessary to develop an automated expert system that is capable of diagnosing the tumor at an earlier stage. We will have more opportunity to investigate and enhance the quality of our work as time passes. Including extra photos is a potential solution. To train a model to be of a higher grade, additional images are necessary. Secondly, one of our near-term objectives is to begin working with 3D photos. Traditional classifiers can achieve even higher levels of precision than those described in the previous two statements. Once a tumor has been identified, more tests are performed to determine whether or not it is malignant. In the not-too-distant future, further deep learning approach variants can be evaluated.

REFERENCES

[1] S. Deepak and P. M. Ameer, “Brain tumor classification using deep CNN features via transfer learning,” Computers in Biology and Medicine, vol. 111, p. 103345, Aug. 2019, doi: 10.1016/j.compbiomed.2019.103345.

[2] P. Afshar, A. Mohammadi, and K. N. Plataniotis, “Brain Tumor Type Classification via Capsule Networks,” IEEE Xplore, Oct. 01, 2018. https://ieeexplore.ieee.org/abstract/document/8451379 (accessed Mar. 22, 2020).

[3] A. Rehman, S. Naz, M. I. Razzak, F. Akram, and M. Imran, “A Deep Learning-Based Framework for Automatic Brain Tumors Classification Using Transfer Learning,” Circuits, Systems, and Signal Processing, vol. 39, no. 2, pp. 757–775, Sep. 2019, doi: 10.1007/s00034-019-01246-3.

[4] N. Abiwinanda, M. Hanif, S. T. Hesaputra, A. Handayani, and T. R. Mengko, “Brain Tumor Classification Using Convolutional Neural Network,” IFMBE Proceedings, pp. 183–189, May 2018, doi: 10.1007/978-981-10-9035-6_33.

[5] M. Sajjad, S. Khan, K. Muhammad, W. Wu, A. Ullah, and S. W. Baik, “Multi-grade brain tumor classification using deep CNN with extensive data augmentation,” Journal of Computational Science, vol. 30, pp. 174–182, Jan. 2019, doi: 10.1016/j.jocs.2018.12.003.

[6] M. Talo, U. B. Baloglu, Ö. Yıldırım, and U. Rajendra Acharya, “Application of deep transfer learning for automated brain abnormality classification using MR images,” Cognitive Systems Research, vol. 54, pp. 176–188, May 2019, doi: 10.1016/j.cogsys.2018.12.007.

[7] J. Cheng, “brain tumor dataset,” figshare, doi: 10.6084/m9.figshare.1512427.v5. Sep. 19, 2019.

[8] T. A. Jemimma and Y. J. Vetharaj, “Watershed Algorithm based DAPP features for Brain Tumor Segmentation and Classification,” 2018 International Conference on Smart Systems and Inventive Technology (ICSSIT), Dec. 2018, doi: 10.1109/icssit.2018.8748436.

[9] N. B. Bahadure, A. K. Ray, and H. P. Thethi, “Comparative Approach of MRI-Based Brain Tumor Segmentation and Classification Using Genetic Algorithm,” Journal of Digital Imaging, vol. 31, no. 4, pp. 477–489, Jan. 2018, doi: 10.1007/s10278-018-0050-6.

[10] S. Arunmozhi, N. S. Madhava Raja, V. Rajinikanth, K. Aparna, and V. Vallinayagam, “Schizophrenia Detection using Brain MRI — A Study with Watershed Algorithm,” 2020 International Conference on System, Computation, Automation and Networking (ICSCAN), Jul. 2020, doi: 10.1109/icscan49426.2020.9262281.

[11] R. D. M N, C. Raju, and R. T. M, “Detection of tumours from MRI scans using Segmentation techniques,” 2021 Second International Conference on Electronics and Sustainable Communication Systems (ICESC), Aug. 2021, doi: 10.1109/icesc51422.2021.9532867.

[12] Kiran, B. D. Parameshachari, and D. S. Sunil Kumar, “SVM Based Brain Tumor Detection and Classification System,” 2022 IEEE 2nd Mysore Sub Section International Conference (MysuruCon), Oct. 2022, doi: 10.1109/mysurucon55714.2022.9972652.

[13] L. Aqhaei, “Employing a Hybrid Technique to Detect Tumor in Medical Images,” 2022 International Conference on Machine Vision and Image Processing (MVIP), Feb. 2022, doi: 10.1109/mvip53647.2022.9738739.

[14] K. Usman and K. Rajpoot, “Brain tumor classification from multi-modality MRI using wavelets and machine learning,” Pattern Analysis and Applications, vol. 20, no. 3, pp. 871–881, Feb. 2017, doi: 10.1007/s10044-017-0597-8. .

[15] P. R, S. P, R. S. A, and V. T, “Brain Tumor Segmentation and Prediction using Fuzzy Neighborhood Learning Approach for 3D MRI Images,” Jul. 2021, doi: 10.21203/rs.3.rs-497725/v1.

[16] F. Dehghani, A. Karimian, and H. Arabi, “Joint brain tumor segmentation from multi MR sequences through a deep convolutional neural network.” 7 Mar 2022, doi.org/10.48550/arXiv.2203.03338

[17] M. Zarinbal, M. H. Fazel Zarandi, I. B. Turksen, and M. Izadi, “A Type-2 Fuzzy Image Processing Expert System for Diagnosing Brain Tumors,” Journal of Medical Systems, vol. 39, no. 10, Aug. 2015, doi: 10.1007/s10916-015-0311-6.

[18] S. Mori and P. B. Barker, “Diffusion magnetic resonance imaging: Its principle and applications,” The Anatomical Record, vol. 257, no. 3, pp. 102–109, Jun. 1999, doi: 3.0.co;2-6">10.1002/(sici)1097-0185(19990615)257:3<102::aid-ar7>3.0.co;2-6.

[19] Shafaf Ibrahim, Noor Elaiza Abdul Khalid,” Image Mosaicing for evalustion of MRI Brain Tissue abnormalities segmentation study”,Int.J.Biology and Biomedical Engineering, issue 4, volume 5, 2011, pp 181-189

[20] S.Karpagam, S.Gowri,”Detection of tumor growth by advanced diameter techni Que using MRI data”, Proc.The world congress of Engineering 2011 Vol WE WEC 2011, London, U.K

[21] M. Zarinbala and M. Izadib, "Systematic image processing for diagnosing brain tumors", Journal of Applied Soft Computing, Volume 11 Issue 1, January 2011.

[22] P. Rajarajeswari, P. Dhanalakshmi, “Intuitionistic fuzzy soft matrix theory and its application in medical diagnosis” Annals of Fuzzy Mathematics and Informatics Volume 7, No. 5, (May 2014), pp. 765-772

[23] Alan Jose, S.Ravi, M.Sambath “Brain Tumor Segmentation Using K-Means Clustering And Fuzzy C-Means Algorithms And Its Area Calculation” International Journal of Innovative Research in Computer and Communication Engineering (An WE SO 3297: 2007 Certified Organization) Vol. 2 , Issue 3 , March 2014

[24] H. Johnson, M. McCormick and L. Ibanez, "The ITK Software Guide", Fourth Edition Insight Software Consortium Updated for ITK version 4.8, July 2015.

[25] K. Delibasis, P. E. Undrill, and G. G. Cameron, “Designing texture filters with genetic algorithms: An application to medical images,” Signal Processing, vol. 57, no. 1, pp. 19–33, Feb. 1997, doi: 10.1016/s0165-1684(96)00183-1.

[26] N. Koul, Dr.G. Kaur and B. Kaur M.Tech "Use of Fuzzy Logic in Various Applications of Digital Image Processing" Department of Electronics Engg Punjabi University, India. ISSN: 2277 128X, Volume 4, Issue 3, March 2014.

[27] R. Debosmit, "Edge Detection in Digital Image Processing." University of Washington: Department of Mathematics, 2013.

[28] A. El Allaoui, "Medical Image Segmentation by MarkerControlled Watershed and Mathematical Morphology," The International journal of Multimedia & Its Applications, vol. 4, no. 3, pp. 1–9, Jun. 2012, doi: 10.5121/ijma.2012.4301.

[29] M. C. Clark, L. O. Hall, D. B. Goldgof, R. Velthuizen, F. R. Murtagh, and M. S. Silbiger, "Automatic tumor segmentation using knowledge-based techniques," IEEE Transactions on Medical Imaging, vol. 17, no. 2, pp. 187–201, Apr. 1998, doi: 10.1109/42.700731.

[30] M. Prastawa, E. Bullitt, and G. Gerig, "Simulation of brain tumors in MR images for evaluation of segmentation efficacy," Medical Image Analysis, vol. 13, no. 2, pp. 297–311, Apr. 2009, doi: 10.1016/j.media.2008.11.002.

[31] M. A. Weber et al., "Diagnostic performance of spectroscopic and perfusion MRI for distinction of brain tumors," Neurology, vol. 66, no. 12, pp. 1899–1906, Jun. 2006, doi: 10.1212/01.wnl.0000219767.49705.9c.

[32] chyzhyk and A. savio, "Feature Extraction from Structural MRI Images Based on VBM Data from Oasis Data Base", The sets of data have been published in the wiki of the GIC's group, 2010.

[33] R. N. Al-Okaili et al., "Intraaxial Brain Masses: MR Imaging–based Diagnostic Strategy—Initial Experience," Radiology, vol. 243, no. 2, pp. 539–550, May 2007, doi: 10.1148/radiol.2432060493.

[34] N. A. Mohamed, M. N. Ahmed, and A. Farag, "Modified fuzzy c-mean in medical image segmentation," 1999 IEEE International Conference on Acoustics, Speech, and Signal Processing. Proceedings. ICASSP99 (Cat. No.99CH36258), 1999, doi: 10.1109/icassp.1999.757579.

[35] Anandgaonkar, G. Sable, "Detection and Identification of Brain Tumor in Brain MR Images Using Fuzzy C-Means Segmentation", International Journal of Advanced Research in Computer and Communication Engineering Vol. 2 , Issue 10, ISSN : 2278-1021, October 2013.

[36] N. Marshkole, B. Singh, A. S Thoke, "Texture And Shape Based Classification Of Brain Tumors Using Linear Vector Quantization", International Journal of Computer Applications, Number 11 - Article 4, September 2011.

[37] W. Bryn "About Brain Tumors", Mawr Avenue, Suite 550 Chicago, IL 60631 The American Brain Tumor Association Website, 2001.

[38] J. C. Silverstein, N. M. Parsad, and V. Tsirline, “Automatic perceptual color map generation for realistic volume visualization,” Journal of Biomedical Informatics, vol. 41, no. 6, pp. 927–935, Dec. 2008, doi: 10.1016/j.jbi.2008.02.008.

[39] Kobbelt, Leif (2006). Vision, Modeling, and Visualization 2006: Proceedings, November 22-24, 2006, Aachen, Germany. IOS Press. p. 185. ISBN 978-3-89838-081-2.

[40] D. Schmidt and R. Odland, “Mirror-Image Reversal of Coronal Computed Tomography Scans,” The Laryngoscope, vol. 114, no. 9, pp. 1562–1565, Sep. 2004, doi: 10.1097/00005537-200409000-00011.

[41] R. C. Gonzalez, R. E. Woods, and B. R. Masters, “Digital Image Processing, Third Edition,” Journal of Biomedical Optics, vol. 14, no. 2, p. 029901, 2009, doi: 10.1117/1.3115362.

[42] J. Jose Furtado , Z. Cai1 & L. Xiaobo," Digital Image Processing: Supervised Classification Using Genetic Algorithm In Matlab Toolbox", University of Geosciences, Hubei, P.R. China, 2010.

[43] A. Pasha, "Morphological Image Processing With Fuzzy Logic", Ankara University, Computer Eng. Dept. 06500, Beşevler Ankara, 2012.

[44] R. C. Gonzalez and R. E. Woods, Digital Image Processing, Third Edition,2008.

[45] Linda G. Shapiro and George C. Stockman (2001): “Computer Vision”, pp 279–325, New Jersey, Prentice-Hall, ISBN 0-13-030796-3.

[46] Barghout, Lauren, and Lawrence W. Lee. "Perceptual information processing system." Paravue Inc. U.S. Patent Application 10/618,543, filed July 11, 2003.

[47] N. Dey, & A. S. Ashour, " Meta-heuristic algorithms in medical image segmentation: a review," Advancements in Applied Metaheuristic Computing, pp.185-203. 2018.

[48] [1]N. M. Zaitoun and M. J. Aqel, “Survey on Image Segmentation Techniques,” Procedia Computer Science, vol. 65, pp. 797–806, 2015, doi: https://doi.org/10.1016/j.procs.2015.09.027.

[49] J. Fritsch, T. Kühnl, and A. Geiger, “A new performance measure and evaluation benchmark for road detection algorithms,” IEEE Xplore, Oct. 01, 2013. https://ieeexplore.ieee.org/stamp/stamp.jsp?tp=&arnumber=6728473.

[50] R. T. Azuma, “A Survey of Augmented Reality,” Presence: Teleoperators and Virtual Environments, vol. 6, no. 4, pp. 355–385, 1997, doi: https://doi.org/10.1162/pres.1997.6.4.355.

[51] X. Wang, R. Girshick, A. Gupta, and K. He, “Non-local Neural Networks,” 2018 IEEE/CVF Conference on Computer Vision and Pattern Recognition, Jun. 2018, doi: https://doi.org/10.1109/cvpr.2018.00813.

[52] [1]B. Caldairou, F. Rousseau, N. Passat, P. Habas, C. Studholme, and C. Heinrich, “A Non-Local Fuzzy Segmentation Method: Application to Brain MRI,” Computer Analysis of Images and Patterns, pp. 606–613, 2009, doi: https://doi.org/10.1007/978-3-642-03767-2_74.

[53] Wang Ya, Zhou Hailin, Ye Jianbing, et al. Color image watershed segmentation based on gradient layered reconstruction [J]. Journal of Image and Graphics, 2017, 22 (6), 807 - 814.

[54] Wang Fuzeng, Wang Xiyuan, Song Jiaqian. Image Segmentation of Marked Watershed Brain Tumor Based on Morphological Filtering [J]. Journal of Ningxia University: Natural Science Edition, 2017, 38 (1): 27 - 32.

[55] Fang Hongping, Fang Kangling, Liu Haixin. Improved H-minima improved watershed stack cell segmentation method [J]. Application Research of Computers, 2016, 33 (5): 1587 - 1590.

[56] Hamaci A, Kucuk N, Karaman K, et al. Tumor-cut: segmentation of brain tumors on contrast enhanced MR images for radiosurgery applications [J]. IEEE Trans on Medical Imaging, 2012, 31 (3): 790 - 804.

[57] Haralick RM, Shanmugam K, Dinstein WE: Textural features for image classification. IEEE Trans Systems Man Cybernet 3:610–621, 1973

[58] S. Patel and R. K. Muthu, "Medical Image Enhancement Using Histogram Processing and Feature Extraction for Cancer Classification," p. 5.

[59] Chung, N. N., Ting, L. L., Hsu, W. C., Lui, L. T., & Wang, P. M. (2004). Impact of magnetic resonance imaging versus CT on nasopharyngeal carcinoma: primary tumor target delineation for radiotherapy. Head & Neck: Journal for the Sciences and Specialties of the Head and Neck, 26(3), 241-246.

[60] Endo, M., Mori, S., Tsunoo, T., Kandatsu, S., Tanada, S., Aradate, H., ... & Kusakabe, M. (2002, November). Development and performance evaluation of the first model of 4D CT-scanner. In 2002 IEEE Nuclear Science Symposium Conference Record (Vol. 3, pp. 1824-1828). IEEE.

[61] Sato, E., Tanaka, E., Mori, H., Kawai, T., Inoue, T., Ogawa, A., ... & Takayama, K. (2006, September). Super-characteristic x-ray generator utilizing a pipe and rod target. In Hard X-Ray and Gamma-Ray Detector Physics and Penetrating Radiation Systems VIII (Vol. 6319, pp. 185-190). SPIE.

[62] T. A. Jemimma, Y. Jacob Vetharaj (ICSSIT 2018). Watershed Algorithm based DAPP features for Brain Tumor Segmentation and Classification CFP18P17-ART; ISBN:978-1-5386-5873-4.